



Transarterial Radioembolization in Hepatocellular Carcinoma

Ramazan Kutlu, Sinan Karatoprak,
and Müge Otlı Karadağ

1 Introduction

Hepatocellular carcinoma (HCC) is one of the deadliest cancers. It is the most common primary liver cancer, sixth most commonly diagnosed, and fourth cause of cancer-related mortality worldwide and represents about 75–85% of primary cancers [1, 2].

There are mainly three modes of treatment: (1) surgical treatments, e.g., resection and transplantation; (2) interventional oncologic liver-directed therapies (ablation, bland embolization, chemoembolization, radioembolization, etc.); and (3) systemic chemotherapy which is indicated for advanced stages [3]. Interventional oncology (IO) has a spectrum of treatment options for the treatment of HCC. In addition to the widely used and well-established IO procedures like radiofrequency ablation and transarterial chemoembolization (TACE), transarterial radioembolization (TARE) with Yttrium-90 (^{90}Y) is becoming an indispensable part of HCC management [4]. Despite these options, the prognosis is poor especially for advanced-stage patients that only one-third of them might benefit from

curative therapies, in addition to the fact that underlying liver diseases predispose to new tumor formation [5].

Although majority of the patients are in intermediate or advanced stages at the time of presentation, therapeutic options are limited, but radioembolization with ^{90}Y , which is a form of localized brachytherapy, has an important role in all stages of HCC with curative intent to palliation [3, 6–8].

2 Radioembolization

The Liver has a dual blood supply, and about 95% of the tumoral blood supply is provided by hepatic artery which makes it possible to embolize the tumor and deliver higher concentration of chemotherapeutics or radiotherapeutics selectively to the liver tumors by avoiding systemic effects [5]. Due to the hypervascularity of hepatic tumors, radioembolization, which could be regarded as a form of brachytherapy, allows localized radiotherapy to liver tumors limiting the dose to the normal parenchyma (Fig. 1) [9, 10]. The isotope ^{90}Y , loaded to glass or resin microspheres, is the most commonly used isotope in TARE [11]. Downstaging the tumor for resection and transplantation; bridging to transplantation, palliation, and maximizing the survival; and intention to treat are the main goals of TARE [12].

R. Kutlu (✉) · S. Karatoprak
Department of Radiology, Inonu University School of
Medicine & Liver Transplantation Institute,
Malatya, Turkey
e-mail: ramazan.kutlu@inonu.edu.tr

M. O. Karadağ
Department of Nuclear Medicine, Malatya Training
and Research Hospital, Malatya, Turkey

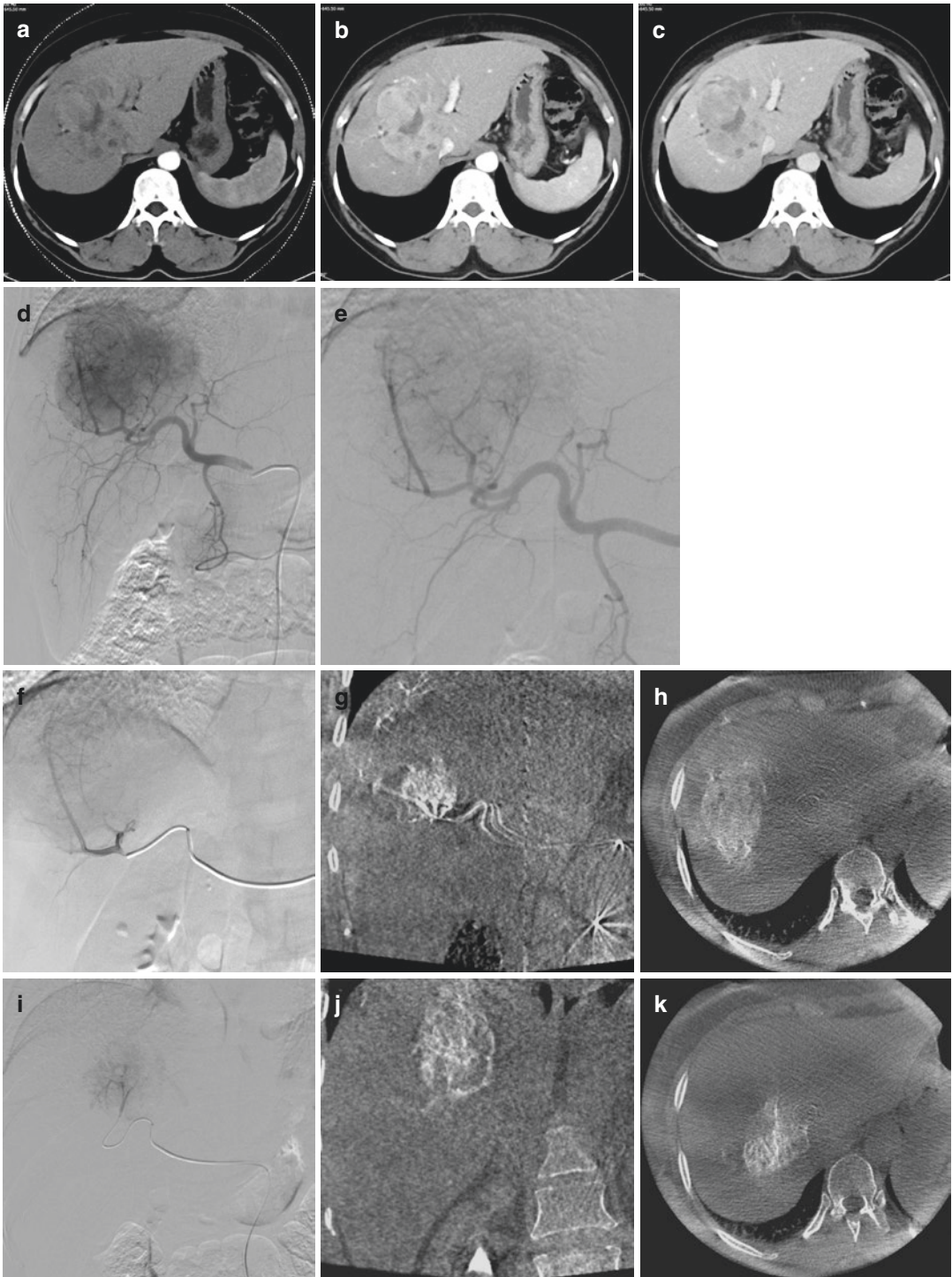


Fig. 1 Axial arterial (a), portal (b), and venous (c) phase CT images show 7 × 4 cm HCC lesion in segment 8. Proper hepatic artery DSA images (d, e) show a hypervascular tumor that has a dual supply from right anterior and posterior sectorial hepatic artery branches. Selective injection DSA images (f, i) and corresponding coronal (g, j) and axial (h, k) cone-beam CT images demonstrate dual

supply of the tumor. PET CT image (l) after administration of two vials of ^{90}Y embedded glass microspheres separately from each feeding artery shows total coverage of the lesion. Corresponding control axial CT images in all phases obtained 3 months after TARE show total necrosis of tumor

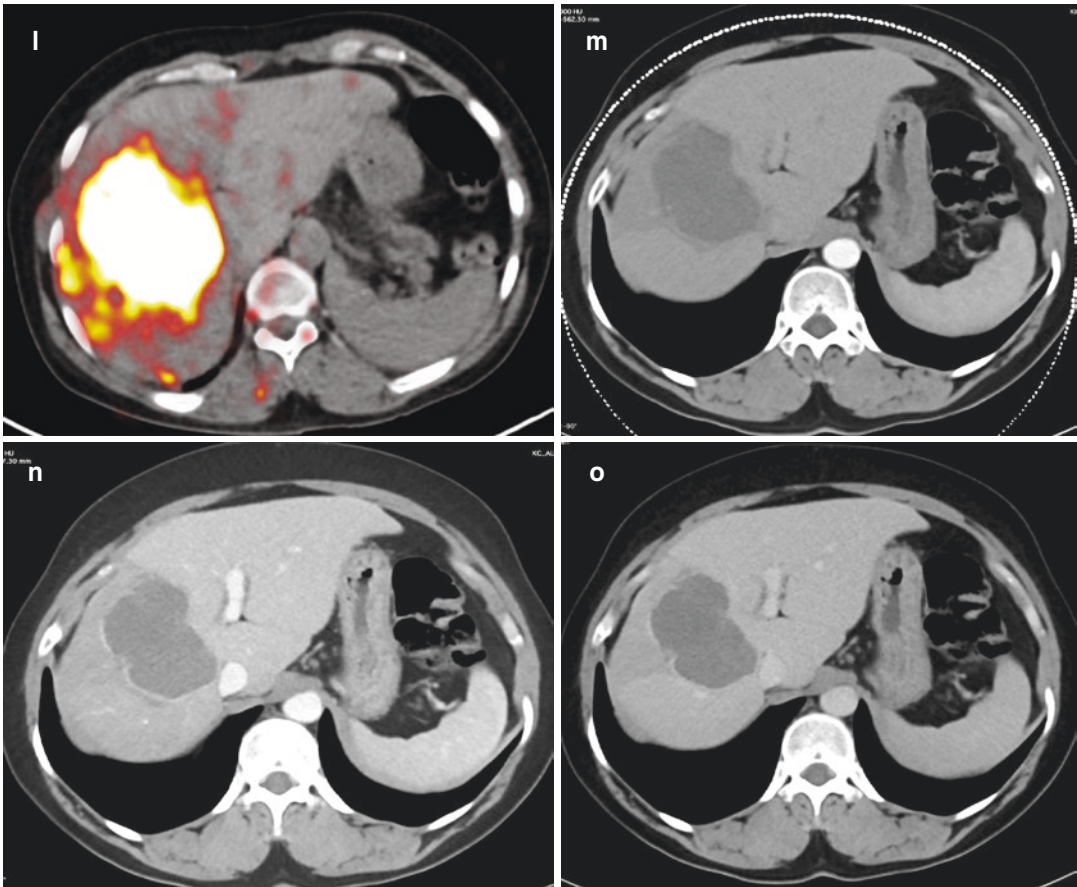


Fig. 1 (continued)

Hepatic arterial variations, flow dynamics, parenchymal reserve, tumoral arterial supply, device-related properties, and activity principles are among the main limiting factors from the point of optimal use of TARE [4]. Ionizing radiation causes unreparable DNA breaks through prolonged exposure that in turn leads to cellular decompensation and apoptosis. The continuous brachytherapy exposure will also damage the cells in different phases of mitosis. TARE also may decrease the intratumoral pressure that helps to improve reoxygenation [4]. TARE has many advantages over other intra-arterial locoregional liver-directed therapies. It is usually an outpatient procedure and could be performed in cases with portal vein thrombosis or compromised portal vein blood flow, and postembolization symptoms are usually minimal. When

compared to TACE, TARE has improved time to progression though no significant difference in mortality [10, 13].

3 Radionuclides and Microspheres for TARE

The type of microspheres can be grouped based on the embedded radioactive isotope (^{90}Y or ^{166}Ho) or microsphere material (resin, glass, or poly-L-lactic acid). These microspheres all have different production processes, physical characteristics, and methods of use. The most important characteristics of the different microsphere types are summarized in Table 1. The comparative properties of the four radionuclides in use in microsphere labeling are given in Table 2.

Table 1 ^{90}Y and ^{166}Ho loaded microsphere characteristics

Isotope	Yttrium-90 (^{90}Y)		Holmium-166(^{166}Ho)
Half-life	64.1 h		26.8 h
Decay product	Zirconium-90 (^{90}Zn)		Erbium-166 (^{166}Er)
Radiation emission	β (max 2.28 MeV)		β (max 1.74 and 1.85 MeV) γ (max 81 and 1.38 keV)
Energy per activity	49.67 J/GBq		15.87 J/GBq
Tissue penetration	2.5 mm mean, 11 mm max		2.5 mm mean, 8.4 mm max
Imaging	PET (internal-pair production) SPECT (bremsstrahlung)		SPECT (γ -imaging) MRI
Material	Glass (ceramic)	Resin	PLLA
Product name	TheraSphere®	SIR-Sphere®	QuiremSphere®
Size	20–30 μm	32.5 \pm 5 μm	20–50 μm
Density	3.3 g/cc	1.6 g/cc	1.4 g/cc
Spheres per vial	1.2 – 8 $\times 10^6$	40 – 80 $\times 10^6$	33 $\times 10^6$
Specific activity per sphere	2500 Bq	40–70 Bq	450 Bq
Max activity per dose	20 GBq	3 GBq	15 GBq
Number of microspheres (for 3 GBq activity)	1.2–8 million	40 million	8–12.5 million
Surrogate particle/scout dose	$^{99\text{m}}\text{Tc}$ -MAA	$^{99\text{m}}\text{Tc}$ -MAA	$^{99\text{m}}\text{Tc}$ -MAA/ ^{166}Ho microspheres
Dosimetry method recommended by manufacturer	MIRD based	BSA method	MIRD based
Handling for dispensing	Not required	Required	Not required
Splitting one vial for two or more patients	Not possible	Possible	Not possible
Specific gravity	High	Low	Low
Embolic effect	Low	Moderate	Moderate

Table 2 Radionuclides used for TARE

Radionuclide	Half-life (hours)	Form and probability of decay	Average/maximum beta emission (MeV)	Average/max range in tissue (mm)	Type of imaging
Y-90	64.2	β^+ positron	0.94/2.20	2.5/12	Bremsstrahlung Planar/SPECT PET
Re-188	17	β γ (155 keV)	0.76/2.12	3.8/11	Planar/SPECT
Ho-166	26.8	β γ (81 keV)	0.66/1.85	2.2/10.2	Planar/SPECT MRG
I-131	482.4 h (8.04 day)	β γ (364 keV)	0.192/0.61	0.8/3	Planar/SPECT MRG

3.1 ^{90}Y Microspheres

Radioactive ^{90}Y can be produced by neutron irradiation of stable Yttrium-89 (^{89}Y) or by chemical separation from the parent isotope Strontium-90 (^{90}Sr), a fusion product of uranium. ^{90}Y is a suitable radionuclide to treat cancer with an appropriate safety profile. It is a nearly pure (99.99%) β -emitter with a half-life of 64.1 hours and decays to stable Zirconium-90 (^{90}Zn). Maximum beta particle (β^-) energy of 2.28 MeV results in an energy release of 49.67 J/GBq and penetration

range in water or soft tissue of 2.5 mm (mean) and 11 mm maximum [10]. Imaging of the radiation emission from ^{90}Y is a challenge due to the absence of γ -radiation emission. SPECT images can only be acquired by the detection of bremsstrahlung, secondary γ -radiation produced by slowing of the beta particles in tissue, a modality with very limited spatial resolution. Actually, ^{90}Y has a minor branch to the first excited state of ^{90}Zn at 1.76 MeV ($0^+ \rightarrow 0^+$ transition). As a result, once in every 32 million (31.86×10^6) decays, an electron-positron (β^- / β^+) pair is created. This

process is called internal-pair production and enables positron-emission detection with PET at high ^{90}Y activities [14].

3.1.1 Glass Microspheres

Glass ^{90}Y -microspheres (Therasphere®, Boston Scientific, Marlborough, MA, USA) are produced by incorporating ^{89}Y oxide into the glass matrix of the microsphere and subsequent activation by neutron bombardment in a nuclear reactor facility [15]. Glass ^{90}Y -microspheres have a relatively high density and a high specific activity per sphere (2500 Bq/sphere) compared with the other microsphere types. Therefore, to administer the same treatment activity, less glass microspheres need to be injected than resin microspheres. As a consequence, the embolic effect is much smaller during injection, so the entire treatment dose can be injected at once with a lower risk of stasis and particle reflux. The microembolic effect of glass microspheres is reported as a significant decrease in tumor enhancement in the cone-beam CT delayed phase images [16]. Main advantages of glass microspheres are no physical manipulation required and due to relatively low number of microspheres given, embolic effects are limited. Therefore, glass microspheres can be also used in patients with portal vein thrombosis; oxygenation is maintained in tumors, and objective responses induced by the irradiation are theoretically improved; and in nearly all cases, the target tissues receive more than 95% of the planned absorbed dose without reaching flow stasis. The specific gravity of glass microspheres is high compared to resin microspheres and may theoretically limit microsphere distribution. The difference in specific gravity is not reported to have a proven effect on clinical outcome [4, 10]. Specific activity is the approximate activity of each microsphere (glass 2500 Bq, resin 75 Bq per microsphere) and is an important factor for dose administration [4]. Moreover, to improve the uniformity of dose distribution within a lesion, the same activity can be injected choosing among different numbers of spheres (i.e., different initial activity) administered after different decay intervals. With crossfire effect, multiple

microspheres create lethal radiation exposure [10]. The low number of spheres may result in inadequate tumor coverage for very large tumors, although the number of spheres can be tailored to the needs by selecting a higher activity vial and by using it later after some degree of decay. With extended shelf-life method, it is possible to allow an increased number of glass microspheres (decayed to the second week of their allowable shelf-life) to be administered for the same planned absorbed dose, therefore allowing better tumoral distribution of the microspheres without causing additional adverse radiation-related events [17]. So, increased embolic load and lowered activity per microsphere theoretically resulted in better tumor coverage and, hence, improved response rates [18].

3.1.2 Resin Microspheres

The production process of resin ^{90}Y -microspheres (SIR-Spheres®, Sirtex Medical Limited, North Sydney, Australia) is different; in this type of microsphere, ^{90}Y cations in solution are chemically incorporated onto the bland microsphere surface by binding to the carboxylic group of the acrylic polymer matrix [19, 20]. Resin microspheres have a much lower density than glass microspheres, which could potentially result in a more distal distribution in the tumor vasculature [21]. Furthermore, the relatively low specific activity requires injection of a higher number of microspheres, approximately 20–80 million. Since this involves a greater embolic effect, stasis of blood flow may occur during administration. Therefore, resin ^{90}Y -microspheres must be administered carefully by hand injection in smaller aliquots, with intervening angiography to reevaluate pace of flow and degree of stasis. Glass and resin microspheres may be used in different or similar tumor types and disease extents, but it remains controversial how the differences in distribution patterns impact treatment efficacy.

The activity vial can be tailored for the patient in the nuclear medicine radiopharmacy if needed. Resin microsphere injection system allows direct monitoring of the treatment because the infusion is performed with alternating injections of sterile

water and contrast medium. In theory, the lower specific gravity is in favor of a better suspension. Main limitation of resin microsphere is the 24 hours of shelf life of the device which is restricting clinical flexibility and patient scheduling. The need for human technical manipulation may result in methodological errors. Resin microspheres are more embolic which might lead to whole-dose delivery failure and transient hypoxia, limiting the effect of radiation.

The main difference between glass spheres and resin spheres is shown in Table 1. Major difference is the activity per sphere; in a glass sphere, activity is about 2500 Bq per sphere with respect to 50 Bq in resin sphere. Glass spheres offer vials between 3 and 20 GBq while resin spheres offer standard 3 GBq vials. Finally, for the same chosen activity, the higher number of resin spheres could provide more uniform dose distribution, with a higher biological effect (toxicity and efficacy). The influence of gravity of glass microsphere can be quoted but never demonstrated on biodistribution [4, 22–26].

3.2 ¹⁶⁶Ho (Holmium-166) Microspheres

The isotope ¹⁶⁶Ho emits both high-energy β-radiation and low-energy γ-radiation. It has a shorter half-life than ⁹⁰Y (26.8 h) and decays with a relatively high dose rate to the stable element Erbium-166 (¹⁶⁶Er). ¹⁶⁶Ho emits β-radiation at two energy levels, maximum 1.74 MeV (48.7%) and 1.85 MeV (50%), with a maximum soft-tissue range of 8.4 mm. The resulting energy release is much lower (15.87 J/GBq) than with ⁹⁰Y; therefore, a larger administered treatment activity is required to achieve the same radiation-absorbed dose in liver tissue [27]. The biodistribution of ¹⁶⁶Ho microspheres can be visualized on SPECT, using the low-energy γ-radiation (81 keV, 6.2%; 1.38 keV, 0.93%), and with magnetic resonance imaging, utilizing the paramagnetic properties of ¹⁶⁶Ho [28]. Holmium microspheres that come with a special management system, unique dosing, and imaging possibilities have become available as well.

Additionally, a scout dose of ¹⁶⁶Ho microspheres can be used instead of ^{99m}Tc-macroaggregated albumin during the preparatory angiography procedure. Thus far, two prospective phase I and phase II clinical studies have been performed on ¹⁶⁶Ho radioembolization in a population of liver metastases from mixed origins. These studies showed that a mean whole-liver dose of 60 Gy is safe and induces tumor response [29, 30].

3.3 ¹⁸⁸Re-Lipiodol (Rhenium-188)

As a generator product, ¹⁸⁸Re has good availability. Unlike the ⁹⁰Y produced in the reactor, it can be obtained from the generator, providing a great advantage for ¹⁸⁸Re, and permits preparation of the ¹⁸⁸Re radiopharmaceutical “on demand” in any hospital radiopharmacy housing the generator. Since it is possible to obtain enough ¹⁸⁸Re from a generator for about 6 months, the production cost is lower when compared to ⁹⁰Y [31]. The physical characteristic is useful for clinical use: a short physical half-life of 16.9 h, high maximal beta energy of 2.1 MeV, and soft-tissue range around 10 mm maximum, similar to ⁹⁰Y. The gamma-emission of 155 keV (15% abundance) allowed pre- and post-therapeutic scans for biodistribution studies and dosimetry [32]. Nowicki et al. investigated the feasibility of ¹⁸⁸Re treatment in patients with primary and metastatic liver tumors, and the median overall survival was 7.1 months; calculated progression-free survival is 5.1 months [33]. Although there are studies similar to this in the literature [34–36], ¹⁸⁸Re microsphere has not yet found widespread use as ⁹⁰Y microsphere.

3.4 ¹³¹I-Lipiodol (Iodine-131 Lipiodol)

¹³¹I is a beta emitting radionuclide with a physical half-life of 8.04 days. The maximum and mean beta particle energies are 0.61 MeV and 0.192 MeV, respectively. Additionally, ¹³¹I emits a principal gamma photon of 364 keV (81% abundance) [37]. The beta radiation of ¹³¹I is

responsible for its therapeutic effects, while gamma radiation makes the distribution of the radiopharmaceutical visible.

Lipiodol is an ester of fatty acids derived from poppy seed oil which is used to diagnose and treat HCC. It was initially used as a radiological contrast medium and was found to have higher uptake in HCC, relative to normal liver tissue [38]. This compound contains an iodine¹²⁷ moiety, which can be exchanged for iodine¹³¹ (I^{131}), to create a compound that delivers targeted, internal, beta, and gamma radiation. Early studies showed that I^{131} lipiodol could induce tumor necrosis and significantly prolong survival in inoperable patients [39]. Treatment with I^{131} lipiodol has been used since the 1990s as palliation for HCC, as it is well-tolerated with few complications or side effects [40, 41].

According to biodistribution data, more than 75% of the I^{131} -lipiodol stays following the arterial administration in the liver, and the remainder reaches the lungs. I^{131} -Lipiodol treatment was at least found effective as chemoembolization and is tolerated much better in the treatment of HCC with portal thrombosis and also as an adjuvant to surgery after the resection of HCCs. In the cases that severe liver dysfunction represents theoretic contraindication for radioembolization as well as for TACE, I^{131} -Lipiodol is an alternative therapy option especially in tumors smaller than 6 cm [42].

Although I^{131} -lipiodol therapy provides an economically viable alternative, long half-life ($t_{1/2} = 8.04$ days), low β -energy [$E_{\beta\max} = 0.61$ MeV (89.3%), 0.33 MeV (7.3%), 0.25 MeV (2.1%)], need for the isolation of patient post-therapy, and high nonspecific lung uptake, which drastically limits the administered dose, make it a less preferred clinical choice [32].

4 Dose and Activity

Dose and activity are two components related to the topic of dosimetry in microsphere therapy. Dose refers to the amount of energy of radiation that is taken up by the tissue within the body and is measured in gray (Gy). Activity refers to the

amount of ionizing radiation and is measured in either curie (Ci) or becquerel (Bq). In microsphere treatment, the term dose (Gy) is used for desired radiation to be delivered to the tumor tissue in the liver, and the term activity (GBq) is used for radiation that is delivered to the target organ (i.e. liver) [43].

TARE naturally targets most tumors as a function of increased vascular density. Since the radiation source is attached to each microsphere, the radiation effects depend on the pattern of their accumulation within the tumor vasculature. This concept requires the distinction between the applied radioactivity and the final tissue exposure when planning a treatment dose as: The dose is the biological effect of radiation measured in gray (Gy) and depends on four factors [4]:

1. Activity: Radioactive decay per unit of time is usually expressed as decrease per second or becquerel (Bq). Most TARE activities are implemented in the range of billions of decays per second or gigabecquerel (GBq).
2. Volume: the amount of tissue in which activity is located.
3. Distribution: Variations in vascular compartments that affect the geographic accumulation of microspheres result in nonuniform irradiation patterns.
4. Radiation susceptibility: radiosensitivity and repair abilities of both tumor and normal parenchyma.

Therefore, activity (GBq) is only one factor in determining the dose (Gy), and the biological effects of TARE should not be overly simplified by assuming uniform distribution of activity within a target volume [44–46].

4.1 Determining Treatment Activity

After the patient is found suitable for treatment in the ^{90}Y microsphere treatment, the stage of determining the appropriate treatment activity is started. There are different methods that differ according to the type of radiomicro-

sphere used for the treatment dose. To date, different methods for the calculation of the amount of radioactivity to be administered have been applied, namely, empirical and dosimetric ones.

There are two commonly used methods to estimate the amount of activity delivered by ^{90}Y microspheres to patients using resin microspheres: a BSA model and a (two-compartment) partition model. An activity detection method generally used for glass microspheres and medical internal radiation dose (MIRD) is referred to as single partition model. Much confusion has arisen as the terms partition model (refers to a two-compartment partition in the use of resin microspheres) and MIRD partition (refers to a single-compartment model used with glass microspheres) have both been abbreviated to the partition model. It is important to notice that the partition model and MIRD partition represent distinct and different methods with significant differences in calculated activity [47, 48].

4.1.1 Empirical Methods

Empirical methods have been tested for resin spheres and are based on a broad estimate of tumor involvement (T) in the liver [tumor volume/(tumor + liver volumes)]. The first empirical method proposed for SIR-Spheres® is based only on T: The larger the tumor burden, the higher the recommended activity in increments of 0.5 GBq per 25% tumor burden.

Empiric Method Calculation

- Tumor <25% of the total mass of the liver by CT scan = use 2 GBq whole-liver delivery.
- Tumor >25% but <50% of liver mass by CT scan = use 2.5 GBq whole-liver delivery.
- Tumor >50% of liver mass by CT scan = 3 GBq for whole-liver delivery.

BSA

The second empirical method proposed for SIR-Spheres® incorporates body surface area (BSA, measured in square meters). Therefore, the activity to be administered is:

$$A(\text{GBq}) = (\text{BSA} - 0,2) + \text{Tumor volume} / \text{Total liver volume}.$$

$$\text{BSA}(\text{m}^2) = 0.20247 \times \text{Height}(\text{m})^{0.725} \times \text{Weight}(\text{kg})^{0.425}.$$

Empirical methods are in use with reported objective responses and low incidence of toxicity. Nevertheless, this approach may intrinsically expose patients to the risk of unnecessary toxicity or tumor underdosage. It must be noted that these methods do not take into account the degree of tumor uptake. Therefore, dosimetric methods should be generally recommended.

The BSA method, to date, has been the most prospectively studied model due to its implementation in several randomized clinical trials [49]. It is also the most frequent method used in dosing resin microspheres. The BSA method generates a hypothetical volume of liver based on the body surface area with dose modulations for tumor burden, large lung shunt percentage, and poor liver function. The main benefit to the BSA method is a generally well-tolerated toxicity profile. The BSA method is otherwise limited by its

lack of anatomic accuracy, disregard of preferential distribution, inability to calculate segmental administrations, and inflexibility to angiosomal demands. As such, some contemporary practices have abandoned the BSA method due to its aforementioned limitations.

The BSA model assumes a relationship between the physical size of the patient and ability to tolerate increasing dosage. The concept that larger patients (not necessarily with larger livers) are more tolerant to increased dosages of ^{90}Y has been shown in the literature [50].

The BSA model was also found to have a lower risk of liver toxicity than the empiric model in the aforementioned cohort of 680 patients treated with resin microspheres, where 21 of 28 cases of radiation-induced liver disease (RILD) occurred from a single center using the empirical model [51].

4.1.2 Partition Method

The purpose of the partition method is to give the maximum dose to the tumor, while the lowest possible dose is given to the liver parenchyma excluding the tumor. This method is based on MIRD theoretical foundations and takes into account tumor and nontumor liver tissue separately. The partition model equation uses patient-specific tumor and liver volumes, along with predetermined T:N from pretreatment ^{99m}Tc -MAA SPECT/CT and/or cone-beam CT (CBCT). Thus, this method represents the most tailored treatment planning algorithm, allowing for accurate estimation of absorbed dose to the tumor, nontarget liver tissue, and lungs. Prior research has shown that treatment planning with the partition model based on ^{99m}Tc MAA SPECT/CT can improve clinical outcomes [52].

Partition Model (Two-Compartment): With this method, SIRT activity calculations are based on the two-compartment model, which allows the amount of radiation delivered to the tumor to be more accurately optimized with an optimum dose of >120 Gy. A higher degree of compatibility is required to arrive at the derivation of equations for activity (and dose) for the lung, normal liver, and tumor. As a result, although this method is theoretically more robust, it has not been widely adopted.

A higher degree of complexity is required to arrive at the derivation of the equations relating to the activity (and dose) to the lung, normal liver, and tumor. As a result, this method, although theoretically more sound, has not been widely adopted [10, 53].

Clinical studies have shown that the background liver parenchyma in cirrhotic patients can tolerate up to 70 Gy of radiation without evidence of radiation-induced hepatitis. Based on this information, the two-compartment partition model was able to optimize the amount of transmitted activity to ensure that tumors receive the minimum amount of radiation needed to cause cellular destruction while protecting the background liver from exposure to excess radiation to minimize the risk of inducing radioembolization-induced liver disease (REILD) [10].

TARE treatment with glass microspheres (Thera-Sphere) uses a simplified single-compartment MIRD model based on the size of the entire liver regardless of the amount of tumor burden with the following formula:

$$\text{Activity GBq} = (D \times m) / 50.$$

D is the dose administered in grays, and m is the mass in kilograms. Using this formula, it can be said that a dose of 50 Gy will be administered to 1 kg of tissue if 1 GBq of ^{90}Y is given. The dose given to the treated mass also depends on the percent residual activity (R) in the vial after treatment and the LSF, which is calculated beforehand. These factors are accounted for in the following formula:

$$D = A \times 50 \times (1 - \text{LSF}) \times (1 - R) / m.$$

The MIRD method is a common model adopted for glass microsphere administration. It requires volumetric calculation of the targeted hepatic tissue and incorrectly assumes a uniform distribution of activity within the volume. Like BSA, the MIRD method does not differentiate the amount of radiation distributed into the tumor and liver parenchyma. While there is abundant safety data to support MIRD utilization with glass microspheres, the specific activity range of this product can vary by orders of magnitude by demand, and the authorized user should be aware of this potential [54].

A practical method based on the hepatopulmonary shunt ratio and liver lobe and/or segment volume and based on a simple internal dosimetric approach is widely used in routine practice to determine therapeutic activity in ^{90}Y glass microspheres. With the software developed to facilitate the calculation in determining the treatment dose, the treatment dose can be calculated practically by using the liver lobe volume where the patient will be treated and the hepatopulmonary shunt ratio obtained from the hepatic artery perfusion scintigraphy data. This software provides the capability to visualize prospective dose distribution and assess the absorbed dose delivered to the target lobe or the tumor and normal tissue. By

allowing for pre- and posttreatment dosimetry, this software can help determine the effectiveness of a patient's ^{90}Y SIRT with confidence. It can be used to interactively tailor the absorbed dose per perfused volume by adjusting the injected activity. The software tools can be customized to a patient's specific tumor presentation and anatomy (personalized dosimetry) (TheraSphere ^{90}Y glass microspheres user's manual).

5 Posttreatment Bremsstrahlung and PET/CT Imaging

Imaging to assess microsphere distribution to the planned liver parenchyma to be sure that there is no nontarget distribution of them after TARE is necessary. Unintended activity leaks could lead to the development of severe complications [55–57].

Post-procedure imaging with bremsstrahlung SPECT and PET/CT can measure defining treatment response and nontarget site embolization. Since ^{90}Y is pure beta emitter, after being administered to the patient, the X-rays created by the Bremsstrahlung effect can be viewed under gamma camera. It is recommended that imaging be done within the first 24 hours after treatment. The ^{90}Y bremsstrahlung SPECT/CT is difficult to measure due to a photopic, collimator detector scattering and lack of septal penetration caused by high-energy bremsstrahlung photons. To quantify, it requires additional compensation that is not readily available in most commercial systems [58–60]. However, the image is still useful in qualitative comparison between delivered and planned deliveries and in controlling extrahepatic uptake [61].

^{90}Y PET/CT is another option for post-therapy imaging. Lhommel et al. [62] showed that imaging ^{90}Y microspheres with PET/CT was feasible, even with the low positron yield of 32 ppm per decay [63]. Studies have shown that time-of-flight (TOF) information helps with quantifying the noisy ^{90}Y PET images [64, 65]. Thus, ^{90}Y post-therapy imaging is capable of providing the

delivered activity distributions with a spatial resolution of a few mm. These can then be converted to absorbed doses, preferably using the voxel-level methods.

Finally, ^{90}Y PET/CT is the most promising modality to replace bremsstrahlung SPECT/CT due to its superior qualitative and quantitative capability. It will play an important role in reorganizing the safety and efficiency profile of radioembolization.

5.1 Anatomy

Variant anatomy is common and reported to be seen in about 40% of population [12]. In order to avoid or at least minimize nontarget embolization of nontumor bearing liver tissue and extrahepatic organs during the TARE, proper knowledge of relevant anatomy is essential [10]. Therefore, a thorough understanding of normal liver anatomy and in particular arterial anatomy together with variations is essential for a successful radioembolization procedure. These variations could be determined before angiography by a properly performed CT examination. A special attention is required for replaced and accessory arteries. They could be the part of dual supply of a tumoral lesion.

In addition to hepatic arterial variations, there are also variations inside the tumor that alter the effectiveness of intra-arterial therapies. Contrast enhancement patterns and Tc-MAA deposition should be evaluated in order to predict intralésional radiation watershed areas that could be managed by increasing either the number of particles or activity [4].

Hepatic tumors are hypervascular and receive supply primarily from hepatic arteries and could also receive parasitic arterial supply from adjacent segments and neighboring organs. Inferior phrenic (Fig. 2), internal mammary (Fig. 3), intercostal, omental, cystic, and adrenal arteries should be evaluated as a potential route of blood supply to the tumors especially in the ones located near the surface of the liver or after intra-arterial therapies [66]. Bare area of the liver is also a frequent site of parasitic supply from



Fig. 2 Selective right renal artery DSA image (a) shows right phrenic artery arising from right renal artery and tumoral supply to the right superior lateral part of tumor. Cone-beam CT coronal (b) and axial (c) images demon-

strate this supply. Control celiac injection DSA image (d) after embolization of right phrenic and also right gastric artery coil embolizations

extrahepatic arteries. Hepatic hilar peribiliary plexus could include numerous small vessels that could be unrecognizable during angiography and due to the progressive increase in intrahepatic arterial resistance which could reverse the hepatopetal flow to the hepatofugal flow resulting in nontarget embolization [67]. Therefore, measures for eliminating this hepatofugal flow should be taken.

In most of the cases, the cystic artery arises from right hepatic artery, and radioembolization could cause radiation-induced necrosis; therefore, whenever possible, microspheres should be

given distal to the cystic artery origin, and if it is not possible, cystic artery could be embolized with Gelfoam on the day of radioembolization (Fig. 4) [68].

Although right gastric artery usually arises from proper hepatic artery, it has a high degree of variation. If microspheres pass through this artery, gastric necrosis, ulceration, and perforation could be seen. Therefore, embolization could be necessary (Fig. 5) [69]. Catheterization could be difficult for embolization, and sometimes embolization of this artery could be done through the left gastric artery [10].

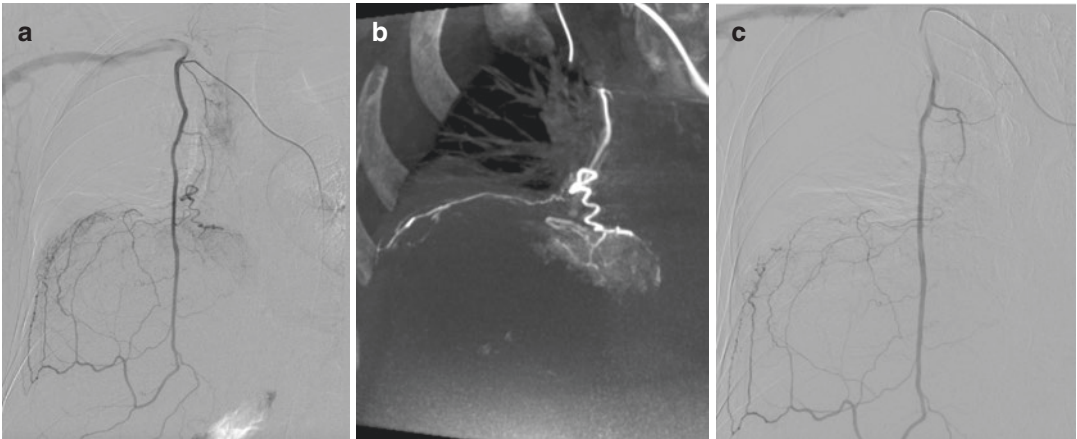


Fig. 3 Selective right internal mammary artery injection (a) and coronal maximum intensity projection cone-beam CT image (b) shows tumoral blood supply to the left

medial superior part of the tumor. Control DSA image after superselective embolization with PVA particles shows cessation of blood supply to the tumor

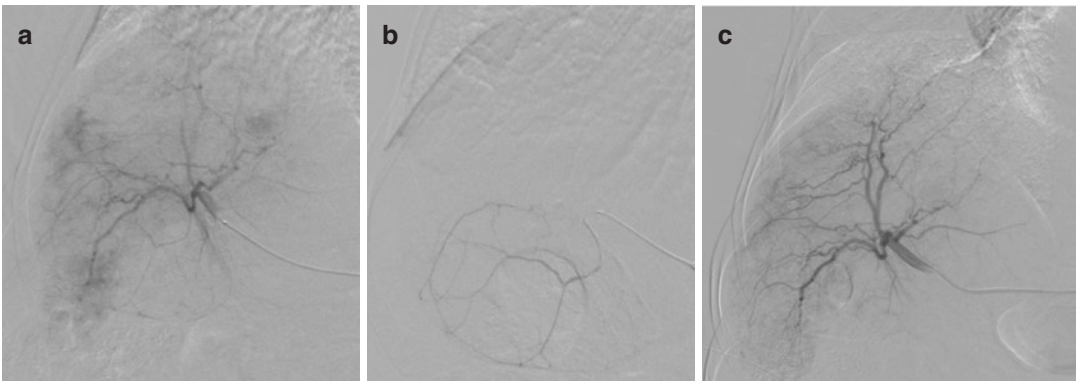


Fig. 4 Selective right hepatic artery injection (a) shows multiple hypervascular tumors and cystic artery originating from the right posterior artery. For right lobar therapy, cystic

artery selectively catheterized (b) and embolized with Gelfoam just before infusion of ^{90}Y . Control right hepatic artery injection (c) shows embolization of cystic artery

In every mapping angiography pancreaticoduodenal arcade should be examined in order to prevent inadvertent pancreatitis, duodenal ulceration, or perforation [10]. When performing embolization in this arcade with a rich collateral vascular network, the possibility of collateralization and recanalization should be considered.

Falciform artery usually arise from the left hepatic artery and could lead to the development of localized, midabdominal wall burning sensation that can last for days or weeks following inadvertent radioembolization. When necessary, it could be embolized or an ice pack could be

placed on the abdomen in order to cause vasoconstriction [70].

Intrahepatic communications between segments provide collateral flow in cases where there is occlusion or compromise of branch hepatic arteries. This feature is used for redistribution and consolidation of flow to tumors, thereby reducing the number of catheter positioning [66]. Embolizations are performed to alter the flow hemodynamics to optimize the administration point of microspheres. It is usually performed during the mapping angiography, and it is better to check them at the day of radioembolization due to the possibility of collateral develop-



Fig. 5 Selective proper hepatic artery injection DSA image (a) shows bilobar disease. For truncal infusion, gastroduodenal artery coil embolized (b). Right gastric artery

arising from proximal left hepatic artery superselectively catheterized (c) and embolized with coils (d)

ment and redistribution. If that is the case, additional embolizations might be required [10].

6 Mapping Angiography

Mapping angiography is performed to assess arterial supply of the tumor to be treated, to determine variant anatomy which could lead to nontarget embolization and embolize them, to consolidate and redistribute arterial supply of tumor to be treated which can also be done during radioembolization, and to calculate lung shunt fraction (LSF) and to simulate radioembo-

lization by administering Tc MAA [4, 12]. The goal of radioembolization is to administer planned required dose to the tumor without damaging normal parenchyma and avoid nontargeted deposition of microspheres into important extrahepatic organs. In order to achieve these goals, hemodynamics of flow to the tumor can be modified by embolization of arteries to redistribute the intrahepatic collaterals to the tumor and to consolidate arteries to administer microspheres by simpler and safer route (Fig. 6) [10, 66, 71]. The assessment of preferential flow is important since it is the primary mechanism of microsphere distribution [4]. Preferential blood flow phenome-

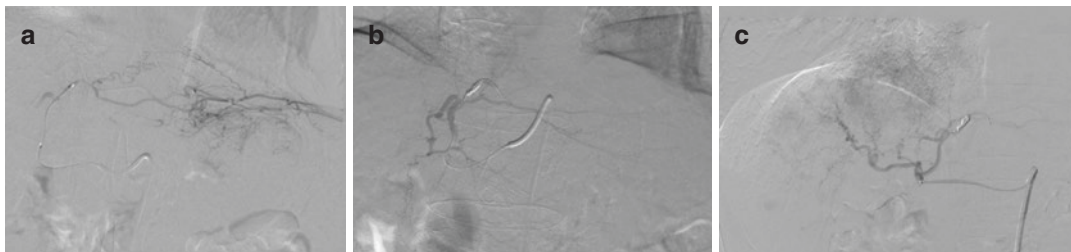


Fig. 6 Selective left hepatic artery injection (a) shows collaterals to the left diaphragm and stomach. These collaterals are embolized with coils to prevent nontarget embolization (b) for truncal infusion (c)

non that generates nonuniform deposition, or compartmentalization, of an embolic substance, allows delivery of ^{90}Y carrying microspheres through the hepatic artery to the tumor [72]. Therefore, one of the reasons of performing mapping angiography is to assess flow dynamics and plan interventions (like embolizations, etc.) to change the dynamics to properly administer and distribute the required dose to the tumors.

In order to optimize vascular dynamics, various permanent and temporary embolization materials, like coils, microplugs, balloons, and Gelfoam, could be used with an intention to decrease nontarget embolization of microspheres and facilitate antegrade flow to the target arteries [10, 12].

MAA is used to assess splanchnic and pulmonary shunting [73]. The size of the albumin microspheres is between 30 and 50 μm which is similar to that of glass or resin microspheres. Due to the density of MAA particles which is almost similar to that of resin microspheres, simulation is better for resin microspheres [74].

Systemic chemotherapies might affect the result of MAA study and eventually biodistribution of ^{90}Y microspheres. Also, they could increase the risk of liver toxicity [75]. Due to hypoxic effects of antiangiogenic drugs, they lead to poor uptake of $^{99\text{m}}\text{Tc}$ -MAA and in turn poor tumor targeting, and therefore they should be discontinued 8 weeks before mapping angiography [75, 76].

6.1 Shunt Reduction

HCC causes the development of functional arteriovenous shunts which is due to the vascular growth factors, neovascularity, complex process

of angiogenesis, and the ongoing autonecrosis/remodeling occurring within tumor microvasculature. Depending on the magnitude of these shunts, microspheres could enter the pulmonary circulation through these shunts causing pneumonitis and fibrosis [7, 10]. Hypervascularity, tumor thrombus in portal and hepatic veins, CT or angiographic findings of shunting to portal or hepatic veins, large tumor burden, and infiltrative disease are among the main risk factors for shunting [7].

If the lung shunt fraction is greater than 20%, there is the possibility of nontarget pulmonary radiation deposition and radiation pneumonitis. The dose of 30 Gy to the lungs is generally accepted as the upper limit of single session of TARE, and 50 Gy is the total upper limit of cumulative absorbed lung radiation dose of repeated TARE [75]. If the hepatopulmonary shunt fraction ratio (HPSFR) is in 10–15% and 15–20%, the activity is decreased by 20% and 40%, respectively. TARE is not performed if the HPSFR is greater than 20% [7, 77].

Shunt reduction procedures, like low-dose TARE, bland embolization, TACE with beads larger than 300 μm , sorafenib administration, chemotherapy, hepatic vein balloon occlusion, variceal embolization, and segmental TARE, are employed in cases with elevated LSF [7, 77].

6.2 Patient Selection

The decision to select patients for radioembolization should be based on a multidisciplinary team that includes nuclear medicine specialists, hepatologists, medical oncologists, radiation oncologists, surgeons (experienced in liver trans-

Table 3 Selection criteria for TARE

Performance	Eastern Cooperative Oncology Group (ECOG) status ≤ 2
Life expectancy	Greater than 3 months
Purpose of procedure	Definitive, bridge to transplantation, palliative
Tumor biology or stage	Advanced-stage or aggressive tumor can be associated with poor prognoses
Liver reserve	Loss of functional liver reserve is associated with the prognosis and benefit of procedure
Hematological parameters	Granulocyte count $\geq 1.5 \times 10^9/L$, platelet $\geq 60 \times 10^9/L$
Renal function	Serum creatinine level < 2.0 mg/dl
Liver function	Serum bilirubin level < 2.0 mg/dl, liver function tests (aspartate aminotransferase, alanine aminotransferase, alkaline phosphatase) should not be above five times of normal level
Tumor size	Tumor involving more than 70% of the liver or 50% of the liver with < 3 mg/dl serum albumin level may have poor prognoses
Pulmonary function	Respiratory function tests should be normal
History of EBRT	Cumulative toxic dose should be regarded

Modified from [4, 74]

plantation), and interventional radiologists [3]. Choosing the treatment modality for HCC depends on some factors such as tumor size, location, morphology (e.g., presence of portal venous invasion, etc.), accompanying comorbidities (e.g., underlying liver disease), and the presence or absence of extrahepatic disease [10]. Selection criteria for radioembolization procedure are summarized in Table 3.

6.3 Indications and Contraindications

The main indications for radioembolization therapy are reduction of size of intrahepatic tumors (downsizing), increasing future liver remnant (FLR) volume, bridging to liver transplantation for HCC, controlling the size of tumor and providing hypertrophy of FLR by radiation lobectomy before resection, delaying progression of advanced HCC (Fig. 7), palliation, and intent to

cure [61]. Applicability in the setting of portal vein thrombosis or invasion, capacity for downstaging or bridging for liver transplantation, facilitation of liver resection by providing hypertrophy of FLR, and the lower incidence of postembolization syndrome are among the advantages of radioembolization [3, 78].

Contraindications of radioembolization are poor liver function (high bilirubin levels and elevated liver function tests, low serum albumin level), renal dysfunction, high lung shunt in mapping angiography, and extrahepatic disease except lymph nodes. Although the serum bilirubin level is required to be below 2 mg/dl, if the tumors can be treated superselectively, radioembolization could be applied to the patients with serum bilirubin levels up to 3 mg/dl. The indications and contraindications of radioembolization are shown in Table 4.

Care should be taken while performing TARE treatment to the patients with poor hepatic function. Total bilirubin is the most widely defined indicator of liver function, and the level of it is desired to be less than 2 mg/dl in patients receiving radioembolization treatment. In patients who undergo bilobar radioembolization therapy, less elevation of bilirubin levels should be a warning about the potential fulminant liver failure. However, patients with moderate hepatic failure can be treated if they are suitable for segmental therapy. Sudden changes from a chronic stable total bilirubin levels may cause sudden decompensation. At this situation, lab values should be rechecked within 10–14 days to assess whether this change is a normal fluctuation or represents a greater hazard [56]. Serum albumin levels provide valuable information for the hepatic function as well. Albumin will often reduce before the increase in total bilirubin, indicating worsening liver reserve and potential loss of liver function [12].

Not all of the HCC patients are eligible for resection or transplantation. Most of the patients are outside the established criteria for liver transplantation. Downstaging means making the patients eligible for resection or transplantation by reducing the size and the number of tumors and tumor marker levels. By this way, patient is brought within the established or expanded crite-

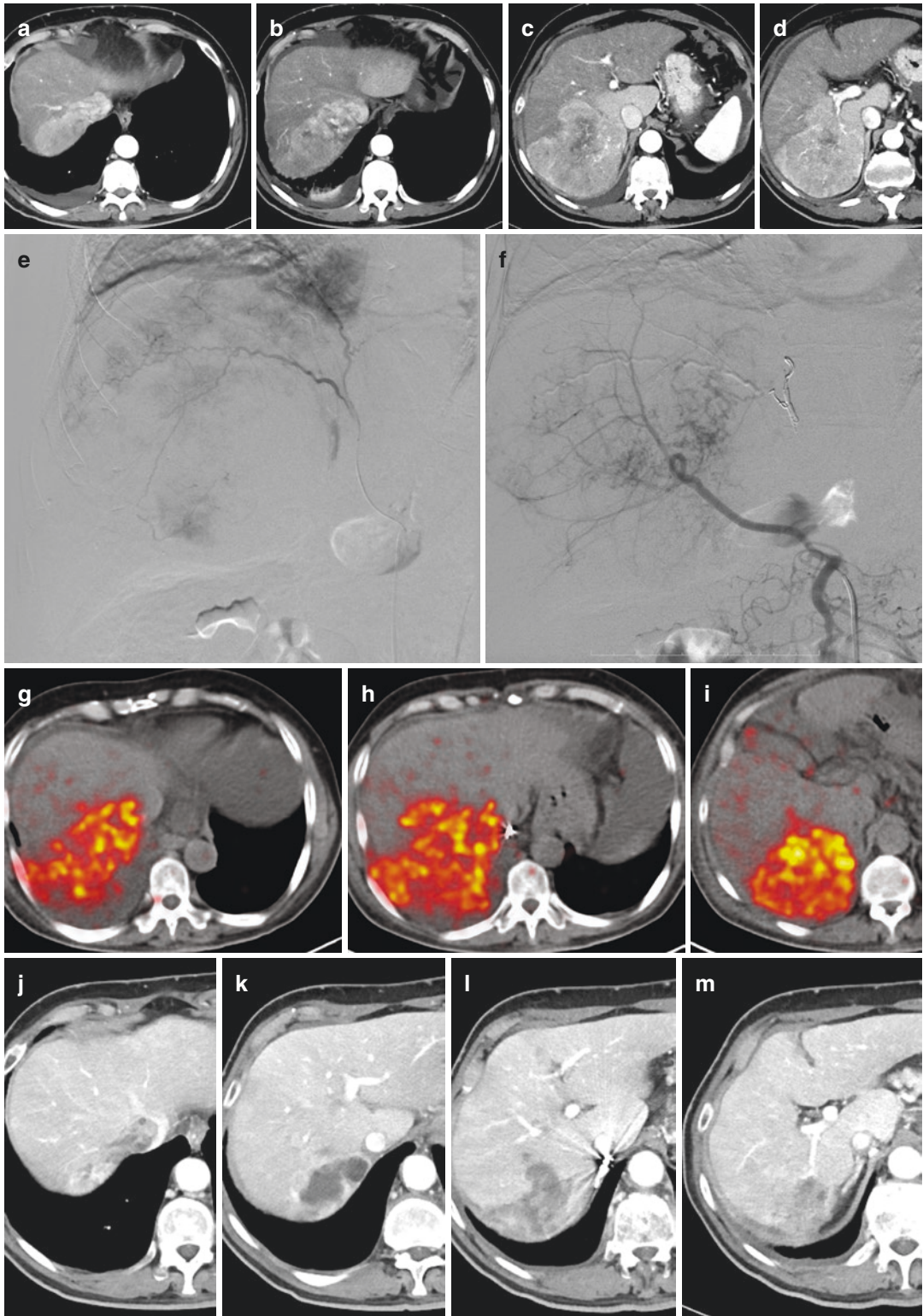


Fig. 7 Consecutive contrast-enhanced axial CT images (a–d) show huge tumor extending to the inferior vena cava. Selective right phrenic artery injection DSA image (e) shows significant tumoral blood supply. ^{90}Y infusion was performed from selectively catheterized replaced

right hepatic artery after embolization of right phrenic artery for consolidation (f). Post-TARE PET images (g–i) show ^{90}Y deposition in tumor. Corresponding control contrast-enhanced axial CT images (j–m) show significant necrosis and decrease in the dimensions of tumor

Table 4 Indications and contraindications for TARE

Indications for radioembolization	
Downsizing	For reducing the tumor size
Increasing FLR	Before liver resection, for increasing the volume of contralateral lobe
Control of tumors	To prevent the increasing of tumor size
Bridging to transplantation	Make suitable the lesions to transplant which are not suitable
To delay progression or palliation	For advanced-stage tumors
Patients with macrovascular invasion	Minimal embolic effect of microspheres
Contraindications for radioembolization	
Poor laboratory values	Serum bilirubin level >2 mg/dl, serum albumin level <2 mg/dl, liver function tests (aspartate aminotransferase, alanine aminotransferase, alkaline phosphatase) above five times of normal level
Renal dysfunction	Serum creatinine level >2 mg/dl
High lung shunt	>30 Gy in single session or >50 Gy in total
Extrahepatic metastasis	Except lymph nodes

ria (Fig. 8). Downstaging by itself is not the only determinant factor for transplantation. In order to understand the tumor biology, there is a need for “test of time” to assess the recurrence or progression of tumor or development of distant metastasis (Fig. 9). Therefore, there should be a “bridging” period until the transplantation whether from cadaveric or live donor [5]. UNOS (United Network for Organ Sharing) and OPTN (Organ Procurement and Transplantation Network) require a progression-free period of at least 6 months from the date of listing [79]. TARE has an important role in both downstaging and bridging. Prolonged response to ⁹⁰Y might be considered having favorable tumor biology and lower recurrence rates [2].

TARE with “curative intent” is usually used for BCLC A patients and solitary tumors with diameters less than 5 cm in unresectable HCC by radiation segmentectomy using higher doses of radiation focally to induce complete pathologic necrosis (Fig. 10) [80].

Radiation lobectomy is another concept for ipsilateral tumor treatment and causing contralateral future liver remnant volume hypertrophy and function similar to portal vein embolization but at a slower rate [81, 82].

Same-day procedure can be applied to some patients with difficult arterial access (such as stenosis, tortuosity, or dissection), with allergy to the contrast, or requiring general anesthesia. This procedure should not be applied to the patients with a low GFR number, vascular invasion, infiltrative tumors, and/or tumor burden more than 50%. Especially patients with macrovascular invasion are more likely to have high degree of lung shunts, so same-day procedure should be strongly avoided [3].

In the presence of recurrence after liver resection, radioembolization is a good alternative treatment option for many patients. However, prior resection may reduce the functional capacity of the liver and can increase the risk of toxicity. It is known that small total liver volume is an independent risk factor of REILD [83, 84]. Decreasing liver volume will cause the absorbed radiation dose to increase relatively and further increase the risk of REILD, too [85]. In spite of all these, in the published series, there is no clearly defined increase of risk for REILD. But in these studies, empiric dose reduction and subtotal liver remnant treatments were applied. In this situation, there is no consensus that the standard ⁹⁰Y dose and therapy may need to be changed after liver resection [86]. So, a conservative treatment strategy should be applied whenever possible. In this condition, postoperative liver volume changes should be taken into account when calculating the patient dose. The aim of the treatment should be keeping the dose of normal liver parenchyma lower than 50 Gy while delivering a therapeutic dose to the tumor [83].

Lobar therapy is more appropriate for multifocal large tumors. Peripherally located solitary tumors are best treated with segmental approach. Tumors in central segments could have dual blood supply from segmental branches from both hepatic arteries.

Portal vein thrombosis is generally accepted as a contraindication for TACE since it is a sign

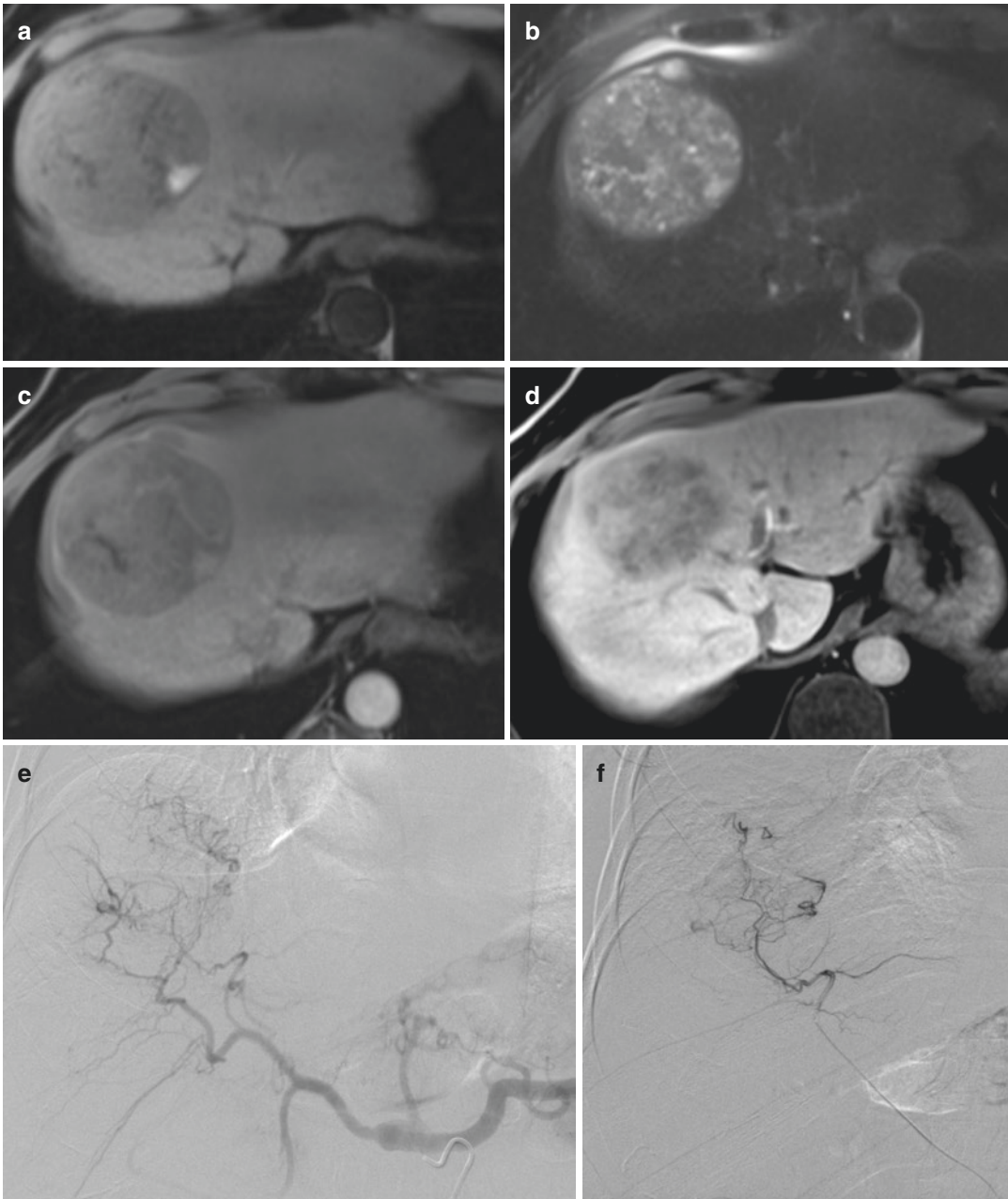


Fig. 8 Axial T1W (a), T2W (b), and T1W contrast-enhanced (c) and liver-specific contrast-enhanced (d) MRI images show an 8 cm HCC lesion in segment 7, 8, and 4. Celiac injection DSA image (e) shows tumoral blood supply from S4 and right hepatic artery. Selective S4 (f) and right hepatic (g) artery injection DSA images and cone-beam CT images (h, i) demonstrate blood supply from S4, S8, and S7 branches. Fusion Tc-MAA CT image (j) shows tumoral coverage. Planar image (k) shows the hepatopulmonary shunt ratio obtained from the hepatic artery perfusion scintigraphy data. Traces are drawn on radiological images to define the liver lobe volume, target volume of the lobe or segment, and tumor

where the patient will be treated (l). The absorbed dose delivered to the target lobe (m) and the absorbed dose delivered to the tumor (n) are calculated. Just before the radioembolization, S4 (o), S5, and S6 arteries (p, q) were embolized with Gelfoam selectively to redistribute and consolidate flow to the tumor. Post-TARE PET CT image (r) demonstrates complete coverage of tumor. Control coronal CT images (s–u) complete necrosis and decrease in diameter of the lesion over 6-month period. After downstaging, patient had live donor liver transplantation. Explant pictures (v, y) show cirrhotic liver and protruding necrotic tumor

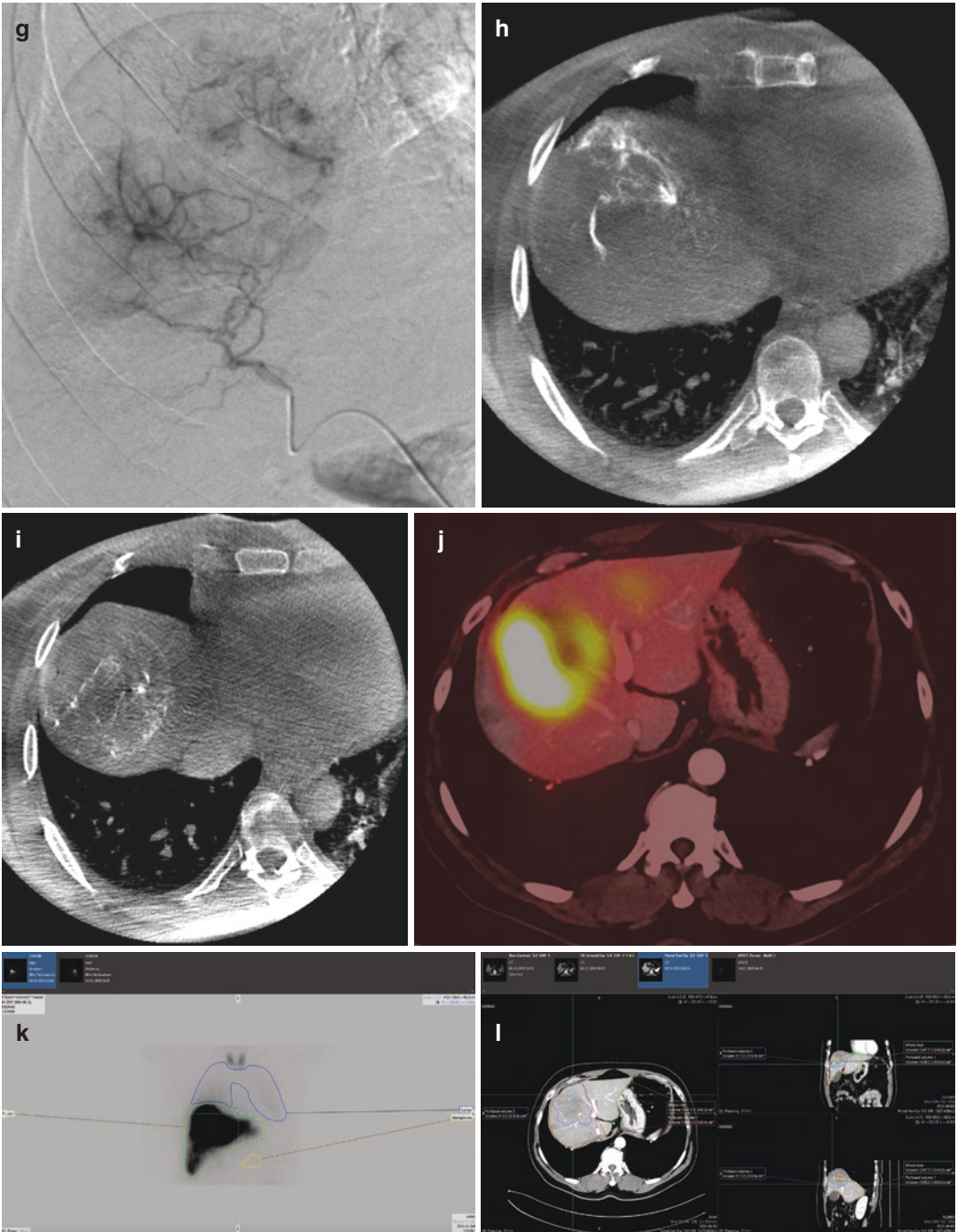


Fig. 8 (continued)

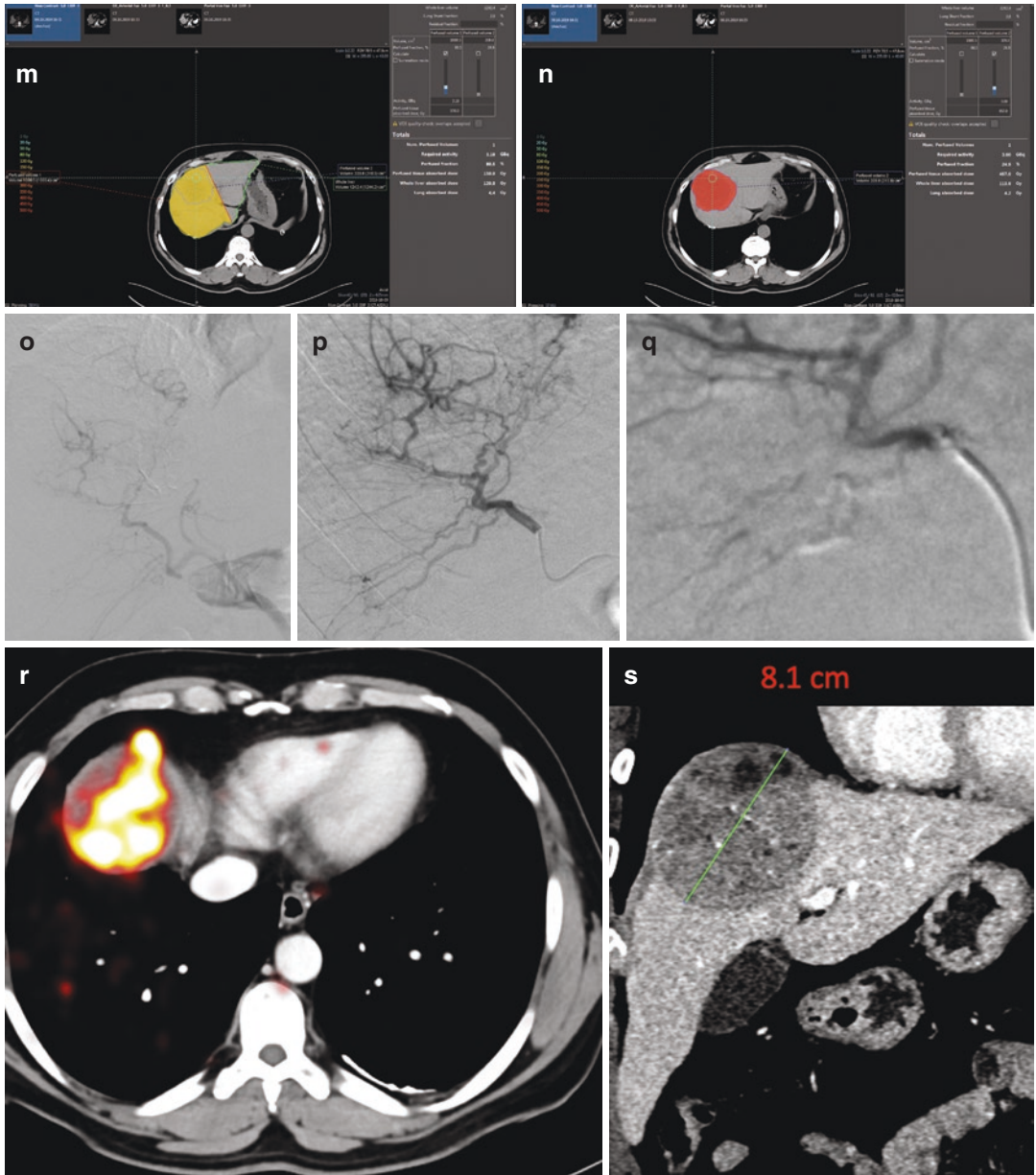


Fig. 8 (continued)

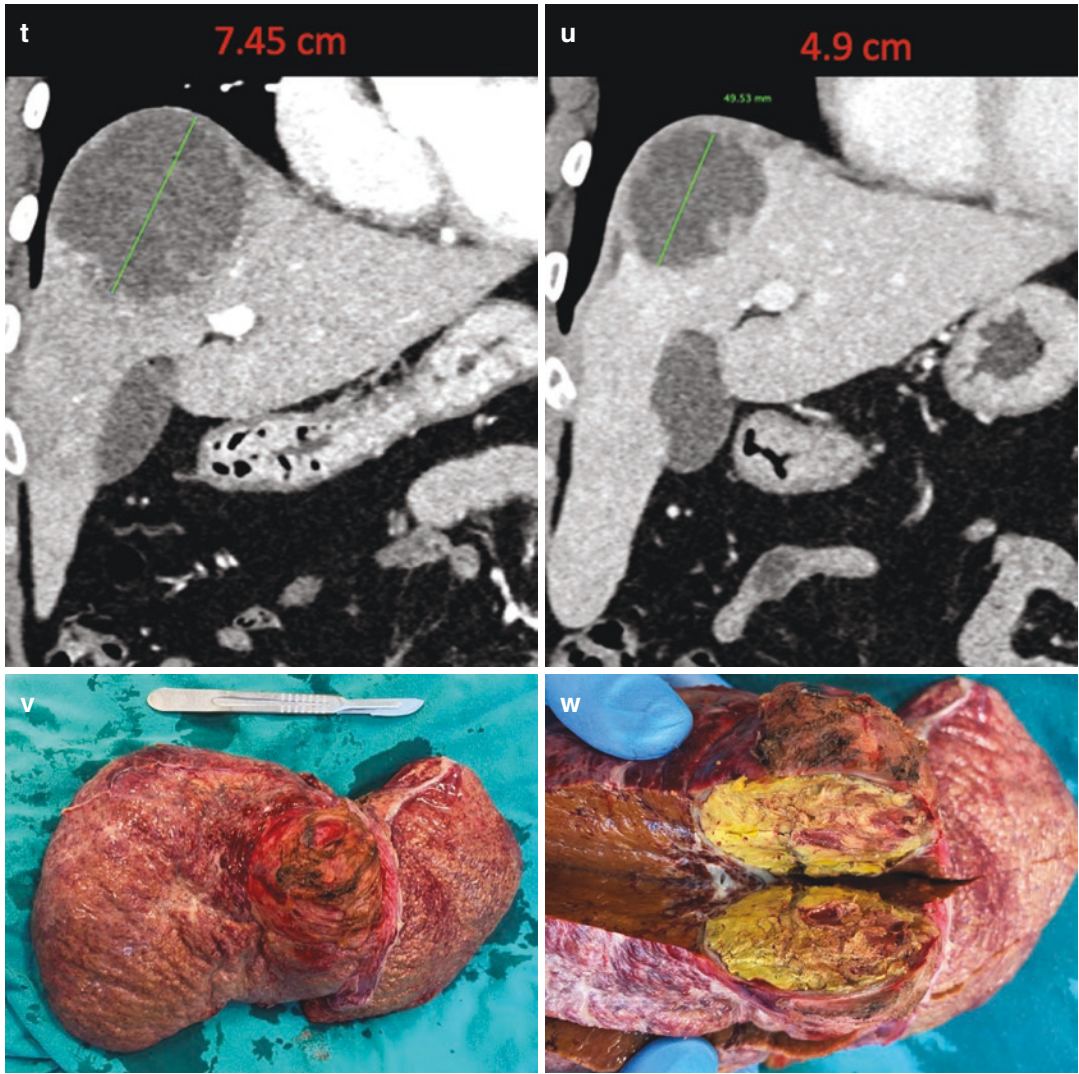


Fig. 8 (continued)

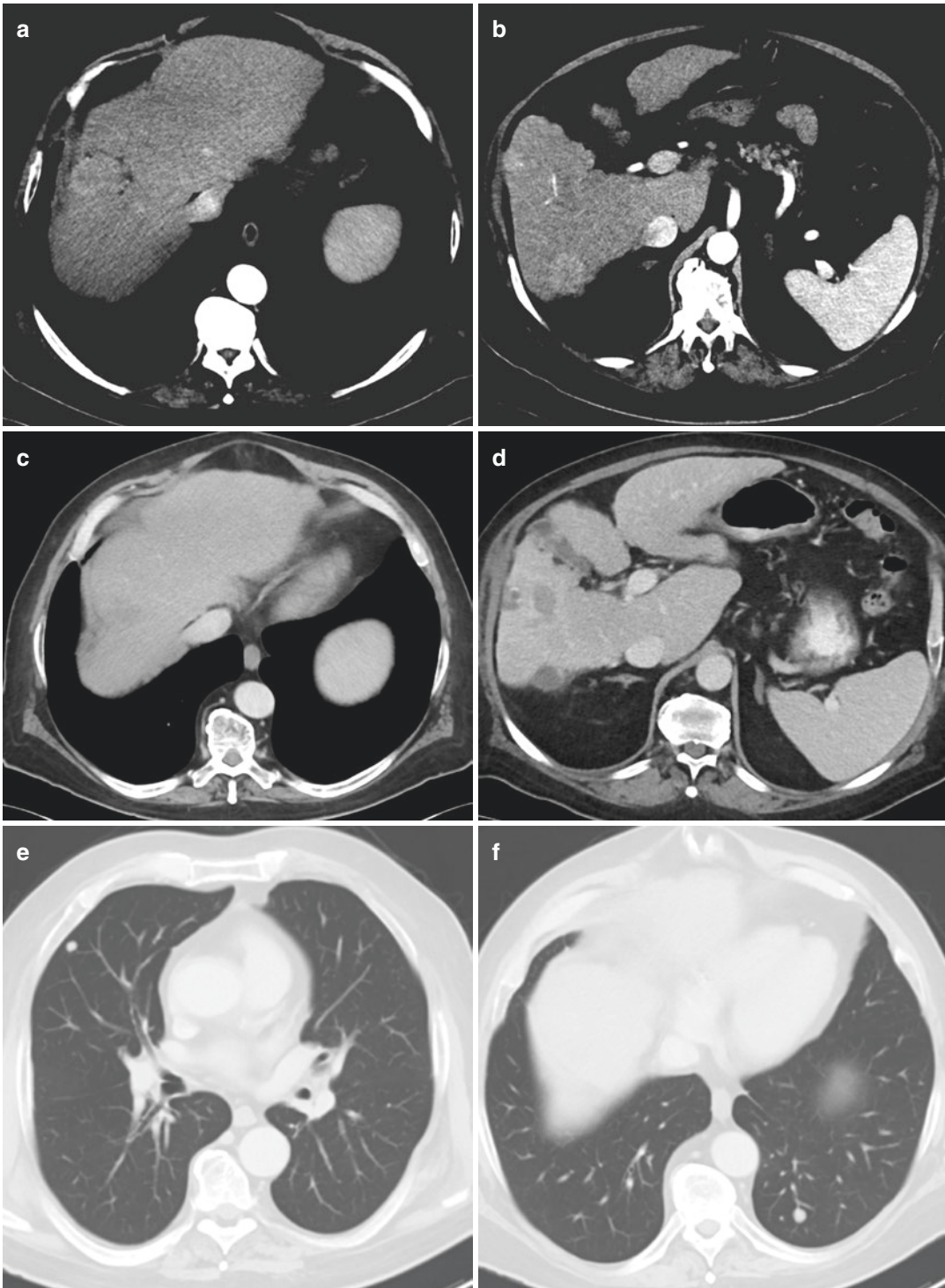


Fig. 9 Axial contrast-enhanced images (**a, b**) show multifocal HCC in the right lobe. Corresponding axial contrast-enhanced CT images (**c, d**) 3 months after TARE demonstrate necrosis of lesions. Although the patient is

downstaged, metastatic lung nodules in both lungs (**e, f**) developed 5 months after TARE, and the patient was delisted from transplantation waiting list

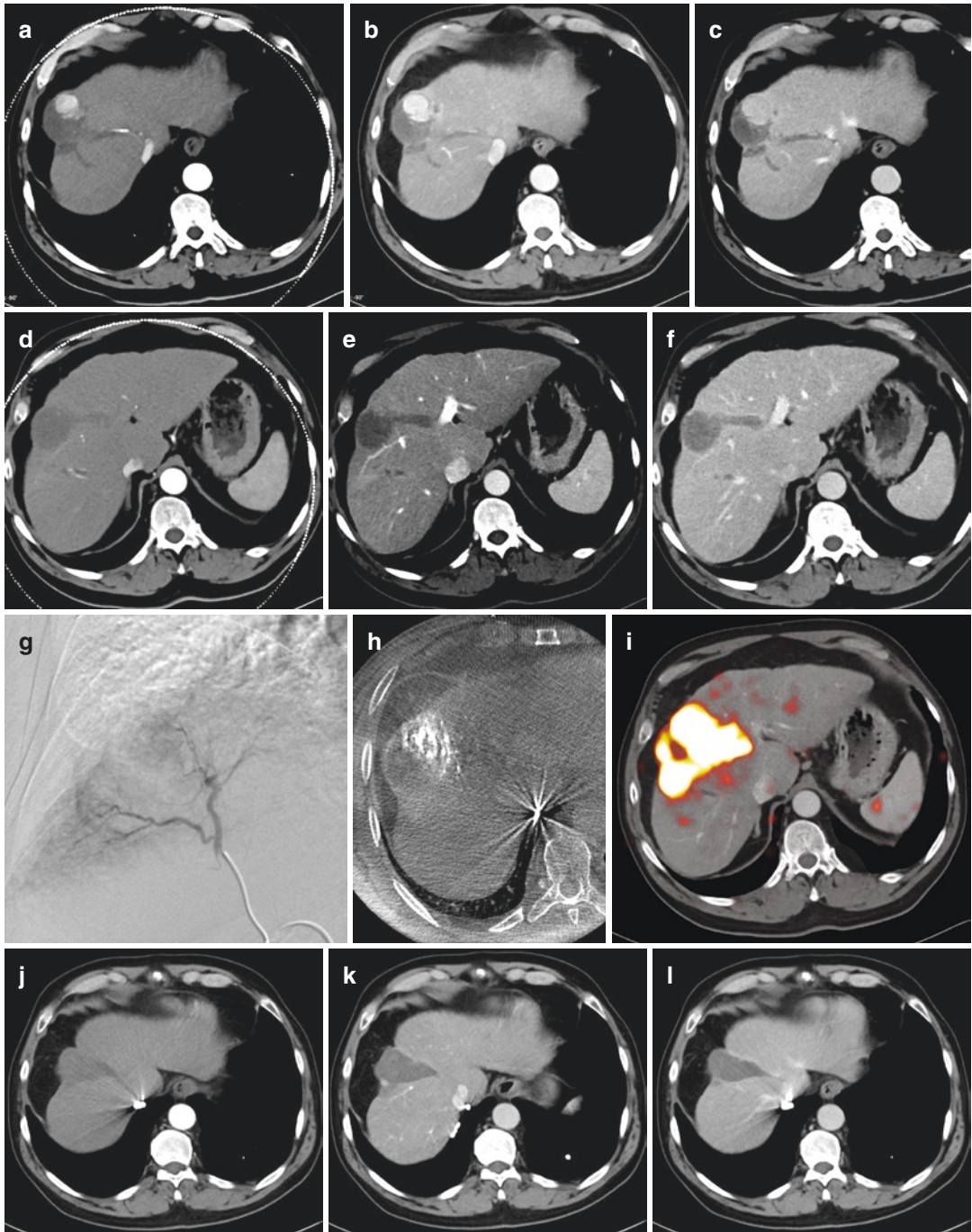


Fig. 10 Axial arterial (a, d), portal (b, e), and venous (c, f) phase CT images at two different levels show an HCC lesion of 4 cm in diameter located in segment 8 with hypervascular nodular part and necrosis. There is also extension to the middle hepatic vein. Superselective injection into the tumoral feeding artery DSA image (g) and axial cone-beam CT image (h) demonstrate wedge-shaped perfusion of the tumor. Post ⁹⁰Y TARE with glass particle

PET CT image (i) shows complete coverage of tumor. Three months after TARE, corresponding axial CT images (j–o) at the same levels demonstrate complete necrosis of the tumor and regression of hepatic vein thrombosis. Coronal reformatted CT images before (p) and after (q) TARE show necrosis of the lesion and regression of the middle hepatic vein thrombus

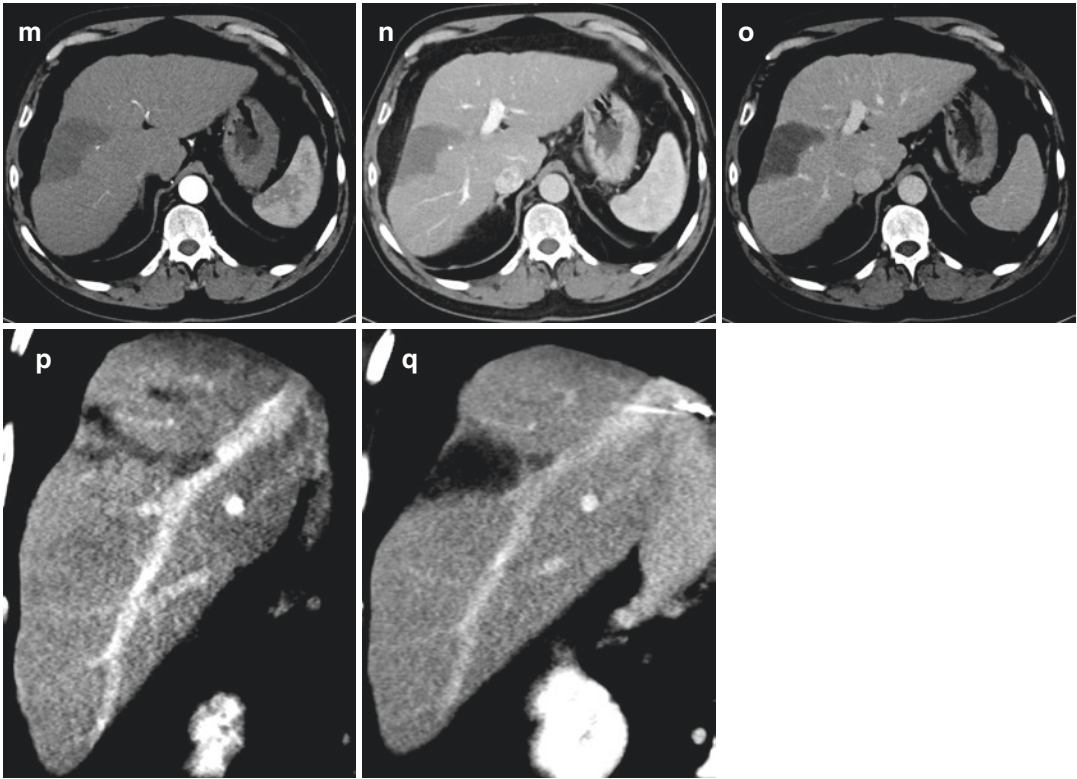


Fig. 10 (continued)

of progressive disease of extensive tumor growth, extrahepatic spread, or progressive functional impairment [6]. Although TACE could be performed by multiple segmental therapies in selected patients, TARE, which has a minimal embolic effect and shown to have favorable response, is a safe alternative in portal vein thrombosis cases, and regression of portal vein thrombus is possible (Fig. 11) [9, 12, 81].

While repeat treatments in unilobar disease appears to be safe, for the bilobar repeat treatments, alternating therapies could be employed [12].

6.4 External Radiotherapy and SBRT

As the liver has low irradiation tolerance, conventional external radiotherapy has a limited place in the treatment of hepatocellular carcinoma. Purpose of the use of external radiation therapy in HCC is mostly palliation of metastasis

such as lymph node, bone, or soft tissue [87–89]. With the developments in technology and the use of three-dimensional conformal radiotherapy (3D-CRT), the use of radiation therapy especially in patients with unresectable HCC has increased. But, although using 3D-CRT, REILD is still a major complication. Especially, in specific locations such as dome of liver (due to radiation pneumonitis) or porta hepatis (due to the risk of major biliary and vascular damage), external beam radiotherapy has limitations [74].

While calculating the dose delivery, nontumoral tissue complications are an important parameter. To minimize the normal tissue complications, respiratory movement must be considered. Delivering the dose in fractions to the tumor may be useful in targeting the radioresistant and radiosensitive malignant cells at different sessions. But, more than one treatment is needed [90].

Due to the technological advances in imaging methods and planning of radiotherapy, stereotac-

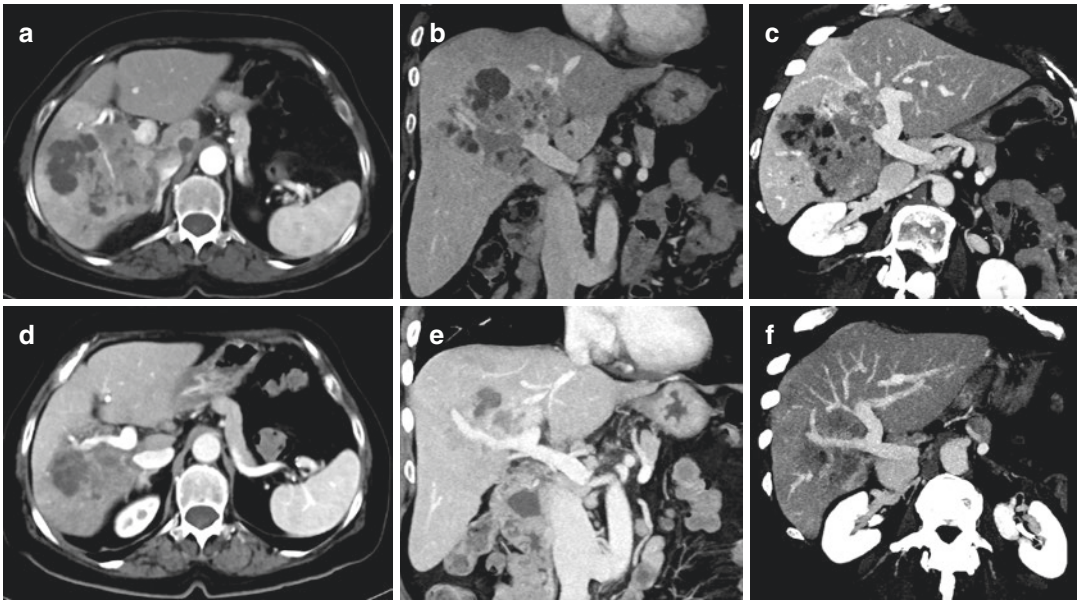


Fig. 11 Contrast-enhanced axial (a), coronal (b), and oblique reformat (c) images show right lobe tumor compressing and invading the right portal vein. Corresponding

control contrast-enhanced images (d–f) show decrease in the size of the tumor and relieve of right portal vein compression and improvement in invasion

tic body radiation therapy (SBRT) which delivers highly conformal radiation therapy with geometric precision has become possible. SBRT has become an effective treatment alternative for early and locally advanced HCC [91–93].

SBRT has recently been recognized as an effective treatment option for nonsurgical localized intrahepatic HCC and included in the 2019 National Comprehensive Cancer Network Guidelines and the practice guideline statement of the American Liver Disease Studies Association [94, 95].

SBRT is used for stabilization and regression in HCC patients as a primary treatment with increasing the median survivals from 11 to 25 months [96–98]. SBRT seems to be safe and efficacious local bridging therapy for patients with local or advanced HCC who are on the waiting list for LT. Also, it can be applied as a primary treatment and can be combined with other locoregional treatment modalities.

In these new techniques, toxic dose is delivered to the tumors while normal liver parenchyma is saved [99]. But, although these advanced targeting techniques are used, liver toxicity after

treatment is still a major problem. So, radioembolization therapy after external radiotherapy should be performed carefully [100].

7 Complications of TARE

TARE is a relatively safe treatment procedure. While a small proportion of patients have experienced mild side effects such as self-limited exhaustion or abdominal pain, TARE is associated with low rates of serious complications. The complications associated with TARE can be divided into three major groups: extrahepatic, intrahepatic, and vascular complications.

7.1 Extrahepatic Complications

Extrahepatic complications of TARE (such as pulmonary, gastrointestinal, esophageal, or pancreatic complications) usually occur because of nontarget embolization and lung shunts which cause radiation-induced pneumonitis due to the high radiation dose to the lungs [101]. Collaterals

between hepatic artery and extrahepatic organs should be identified during mapping angiography and should be embolized prophylactically before TARE in order not to cause nontarget embolization.

7.1.1 Radiation-Induced Lung Disease

There is limited information about radiation-induced lung disease after radioembolization treatment. In a review of 515 patients by Kennedy et al., the incidence of RILD was found to be 4%. Of these, 75% was treated single session whole-liver therapy by using empirical dosimetry. In current practice, empirical dosimetry method is no longer used [51]. The effect of the microspheres on the lung parenchyma is due to arteriovenous shunts, which are commonly seen in HCC [102]. During radioembolization, some of the ^{90}Y passes to the lung because of these intratumoral arteriovenous shunts. Mapping angiography with $^{99\text{m}}\text{Tc}$ MAA minimizes the risk of RILD by evaluating lung shunts and calculating treatment dose. The cases in the literature describe life-threatening disease which includes pathologically acute-subacute interstitial pneumonitis. In these patients, increasing dyspnea and restrictive lung disease developed in 1–6 months after radioembolization [103]. It is important to exclude the other reasons of dyspnea in patients who present with shortness of breath. There is no evidence-based treatment for RILD. Supportive treatment with oxygen supplementation and intravenous steroid can be performed [8].

7.1.2 Gastrointestinal Complications

Nontarget infusion of microspheres to the gastrointestinal organs might cause ulceration or perforation in these organs. In a review with 39 studies by Naymagon et al., mean incidence of gastric ulceration after radioembolization was found to be 4.8% [104]. Approximately 5 weeks after radioembolization, these patients experience abdominal pain, nausea, anorexia, and vomiting [105]. Ulceration of the stomach or duodenum which is induced by Yttrium-90 may not respond to medical therapy. So, surgery may be needed. To prevent radioembolization-associated ulcer-

ation, mapping angiography should be performed carefully and coil embolization should be done if necessary.

If the microspheres spread into the pancreatic vessels, radiation-induced pancreatitis may occur. This type of pancreatitis usually affects the head of the pancreas. This complication can be very painful for the patient and leads to a prolonged hospitalization, food restriction, and i.v. treatment.

Although it is theoretical, damage of attenuated radiation to the organs adjacent to the liver (such as the colon, duodenum, or stomach) may be possible as gastritis or enteritis. Another side effect of attenuated radiation may occur in the right hemithorax as pleural effusion [101].

7.1.3 Radiation-Induced Cholecystitis

Although it is rare, ^{90}Y carrying microspheres could enter into the cystic artery and perforators from the hepatic parenchyma or into the gastroduodenal artery branches that supply gallbladder and then cause mucosal injury and ischemia. In order to prevent radiation-induced cholecystitis, infusion distal to the cystic artery is advised. In cases where this is not possible due to necessary flow dynamics or anatomic location, prophylactic embolization, usually with temporary agents, could be employed. If radiation cholecystitis develops, most cases are followed conservatively. However, if there is perforation or emphysematous cholecystitis, then cholecystectomy or percutaneous cholecystostomy may be needed (Fig. 12) [101, 106, 107].

7.1.4 Bile Duct Complications

Intra- and extrahepatic biliary complications after TARE are associated with the embolic effect and necrosis of the biliary ducts due to radiation. Unlike normal liver parenchyma, the intrahepatic bile ducts have only single feeding artery which arises from the hepatic arterial branches as a vascular plexus (peribiliary capillary plexus) around the bile ducts. The diameter of the vessels in this plexus is the same as ^{90}Y embedded microspheres; therefore, after TARE, ischemia may develop in the bile ducts [108]. In a study with 327 patients who underwent TARE by Atassi

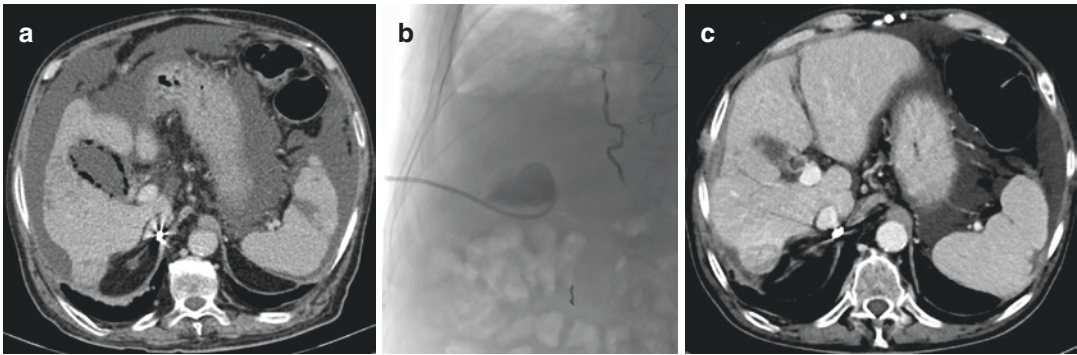


Fig. 12 Contrast-enhanced axial CT image (a) after TARE shows ascites and air in the gallbladder wall (emphysematous cholecystitis). Spot image (b) obtained after placement of percutaneous cholecystostomy shows

the drainage catheter and embolization coils in right phrenic artery. Control contrast-enhanced axial CT image (c) after removal of drainage catheter shows resolution of cholecystitis and ascites

et al., the rate of biliary sequelae was approximately 10%. Less than 2% of patients needed biliary interventions. The most common biliary complications were biliary stricture and necrosis. Most of biliary interventions employed for these complications are drainage of bilomas and abscesses and percutaneous cholecystostomy for radiation cholecystitis. Biliary necrosis was less common in patients with primary HCC than in patients with metastatic liver lesions. This may be due to the hypertrophy of the peribiliary vascular plexus and history of chemotherapy of patients with metastatic tumors [109]. Damage in the bile ducts can take several forms such as biloma cavities or dilatation of the bile ducts. The reason of the biloma cavities can be the necrosis of the peripheral bile ducts with leakage due to the damage of vascular plexus which supplies bile ducts [110, 111]. Treatment of biliary damage after radioembolization is usually conservative. Percutaneous drainage for bilomas or abscesses, balloon dilation, or stents for strictures can be applied. Surgery may be necessary in very rare cases.

7.1.5 Radioembolization-Induced Liver Disease (REILD)

Sangro et al. [50] first used the term of REILD which refers to a collection of symptoms resulting from progressive liver decompensation related to radioembolization. Findings of the REILD are jaundice, ascites, high serum bilirubin

levels, and low serum albumin level, and incidence of it is nearly 5% [85]. REILD typically presents with patterns of sinusoidal obstruction as veno-occlusive disease. Supportive treatment is applied to these patients. While the syndrome can be self-limited, liver failure and death can be seen in serious cases [50].

All transarterial embolic therapies could cause liver toxicity that its degree of damage depends on many factors like dose, particle size, baseline liver reserve, and tumor to liver perfusion. The calculation of actual dose of normal liver parenchyma is difficult since microspheres distribute inhomogeneously. Functional liver reserve and regenerative function are the two main determinants of liver toxicity. Cirrhosis, previous chemotherapies and locoregional therapies, resection, etc. all affect the functional reserve and regenerative capacity. In almost all the patients that underwent radioembolization treatment with ^{90}Y , some degree of liver toxicity is seen.

Liver-dependent factors such as infiltrative type of HCC (volume of the tumor 50% of total liver volume), serum liver transaminases levels greater than five times the normal value, serum albumin level <3 g/dl, and total serum bilirubin level >2 mg/dl strongly associated with a 3-month mortality. The bilirubin level is the best indicator for REILD [10].

Although serious liver toxicity associated with radioembolization is rare, if it develops, it

can be divided into early and late stages. Acute liver toxicity occurs in 2–16 weeks after treatment with no tumor progression or biliary obstruction [112].

Chronic toxicity can be seen in months or years after treatment. So, the rate of chronic toxicity is not known well yet. The mechanism of chronic toxicity is thought to be associated with radiation-induced fibrosis. It presents with atrophy of the liver and findings of portal hypertension [113, 114].

REILD is so rare after the first TARE therapy. If there is no lesion in the contralateral lobe, the second session can be tolerated as well. But the cumulative dose of the liver increases the risk, so prior whole-liver therapy is an important risk factor for REILD. If the tumoral lesions could be catheterized selectively, patients with large tumors can be treated safely even when they have other risk factors for toxicity [85]. Instead of whole-liver therapy, sequential lobar treatment can be performed to allow the contralateral lobe for regeneration with an interval of 4–6 weeks. However, caution should be exercised when considering sequential treatments because REILD may occur in 16 weeks after first procedure. So, the absence of clinical deterioration in 4–6 weeks after treatment should not be seen as conclusive evidence that additional therapy is safe [115].

For the mild cases, current standard of treatment includes diuretics and long-term high-dose steroids. For more serious and acute cases, long-term low-dose heparin, ursodeoxycholic acid, and pentoxifylline can be added to treatment [10].

7.1.6 Post Radioembolization Syndrome

In post radioembolization syndrome, symptoms such as fever, fatigue, nausea, vomiting, and anorexia are seen. The incidence of it has been defined as significantly less than the postembolization syndrome encountered after TACE. Post radioembolization syndrome is usually self-limited. Some patients may need symptomatic treatment and hospitalization. Single-dose steroids can be given preprocedurally [8].

7.2 Vascular Complications

TARE treatment has the same risks of vascular complications with other intra-arterial procedures. Hematoma or pseudoaneurysm at the access site or arterial dissections can be seen during therapy. The risk of vascular injury increases in patients who have previously received chemotherapy [18].

8 Radiologic Follow-Up

The aim of the follow up is the evaluation of the response or disease progression. Four-phase dynamic contrast-enhanced CT or multiphase dynamic contrast-enhanced MRI is performed after 4–8 weeks following TARE procedure to evaluate the response to the therapy. To avoid the misinterpretation of reversible or transient findings, intervals of follow-up imaging is not performed earlier [56, 116]. The most common transient finding on follow-up CT images is reduced density at the site where microspheres accumulate. These findings are thought to be due to edema, congestion, or microinfarction in the treated areas [56]. After the first radiological study, patients are followed with scans every 3 months.

According to the guidelines of the World Health Organization (WHO) and the Response Evaluation Criteria in Solid Tumors (RECIST) group, the most important indicator of a successful treatment response is reduction in tumor size [117]. However, necrosis, cystic degeneration, hemorrhage, or edema can cause the increasing in tumor size. The European Association for the Study of the Liver (EASL) necrosis criteria are also used to evaluate necrosis that develops in tumors [118]. According to a recent study, use of combined size and necrosis criteria is more accurate than the use of size criteria alone in evaluating the response to ⁹⁰Y treatment [119]. Therefore, the indicators which can show tumor necrosis such as tumor vascularity, 18-fluorodeoxyglucose uptake on PET-CT, volume of tumor (viable tumor burden), diffusion weighted MRI, and serum tumor markers (serum AFP level) should be evaluated for tumor response. Functional MRI

may play a role in detecting tumor response earlier [120]. It may take 6–9 months to achieve maximum response (totally devascularization with no recurrence). Serial imaging together with laboratory examinations allows proper follow-up of treated patients for the response assessment. Follow-up imaging also helps to evaluate patients who were downstaged or in bridging period for the possible recurrences.

9 Conclusion

Interventional oncologic approaches broaden the treatment options for HCC. TARE is a safe and effective option for selected group of patients who are not suitable for surgery or other locoregional interventional treatments or patients with failed interventions. It has a proven effect in downstaging and bridging. TARE has an important role in every stage of HCC, and the technical developments and improvements in dose-related issues will positively affect the outcomes of patients with HCC.

References

1. Singal AG, Lampertico P, Nahon P. Epidemiology and surveillance for hepatocellular carcinoma: new trends. *J Hepatol.* 2020;72(2):250–61.
2. Tabone M, Calvo A, Russolillo N, Langella S, Carbonatto P, Lo Tesoriere R, et al. Downstaging unresectable hepatocellular carcinoma by radioembolization using 90-yttrium resin microspheres: a single center experience. *J Gastrointest Oncol.* 2020;11(1):84–90.
3. Gabr A, Ali R, Al Asadi A, Mora R, Mouli S, Riaz A, et al. Technical aspects and practical approach toward same-day Y90 radioembolization in the management of hepatocellular carcinoma. *Tech Vasc Interv Radiol.* 2019;22(2):93–9.
4. Toskich BB, Liu DM. Y90 radioembolization dosimetry: concepts for the interventional radiologist. *Tech Vasc Interv Radiol.* 2019;22(2):100–11.
5. Kutlu R, Karatoprak S. Radioembolization for hepatocellular carcinoma in downstaging and bridging for liver transplantation. *J Gastrointest Cancer.* 2020;51(4):1157–64.
6. Helmberger T. HCC. Radioembolization combined with other therapeutic local and systemic treatment. In: Bilbao JI, Reiser MF, editors. *Liver radioembolization with 90Y microspheres.* Medical radiology. Berlin, Heidelberg: Springer Berlin Heidelberg; 2013. p. 119–27.
7. Schiro BJ, Amour ES, Harnain C, Gandhi RT. Management of high hepatopulmonary shunts in the setting of Y90 radioembolization. *Tech Vasc Interv Radiol.* 2019;22(2):58–62.
8. Titano JJ, Kim E, Patel RS. Yttrium-90 complications: prevention and management. *Tech Vasc Interv Radiol.* 2019;22(2):87–92.
9. Gabr A, Kallini JR, Salem R. Radioembolization for liver tumors. In: Jarnagin WR, editor. *Blumgart's surgery of the liver, biliary tract and pancreas, 2-volume set.* Elsevier; 2017. p. 1417–25.e2.
10. Thakor AS, Eftekhari A, Lee EW, Klass D, Liu D. Hepatocellular carcinoma: radioembolization. In: Ganguli S, Gandhi RT, Faintuch S, editors. *Practical guides in interventional radiology interventional oncology.* New York: Thieme; 2016. p. 84–107.
11. Lewandowski RJ, Riaz A, Ryu RK, Mulcahy MF, Sato KT, Kulik LM, et al. Optimization of radioembolic effect with extended-shelf-life yttrium-90 microspheres: results from a pilot study. *J Vasc Interv Radiol.* 2009;20(12):1557–63.
12. Klimkowski S, Baker JC, Brown DB. Red flags, pitfalls, and cautions in Y90 radiotherapy. *Tech Vasc Interv Radiol.* 2019;22(2):63–9.
13. Zori AG, Ismael MN, Limaye AR, Firpi R, Morelli G, Soldevila-Pico C, et al. Locoregional therapy protocols with and without radioembolization for hepatocellular carcinoma as bridge to liver transplantation. *Am J Clin Oncol.* 2020;43(5):325–33.
14. D'Arienzo M. Emission of β^+ particles via internal pair production in the $0^+ - 0^+$ transition of ^{90}Zr : historical background and current applications in nuclear medicine imaging. *Atoms.* 2013;1(1):2–12.
15. Wollner I, Knutsen C, Smith P, Prieskorn D, Chrisp C, Andrews J, et al. Effects of hepatic arterial yttrium 90 glass microspheres in dogs. *Cancer.* 1988;61(7):1336–44.
16. Pellerin O, Lin MD, Bhagat N, Shao WB, Geschwind JF. Can C-arm cone-beam CT detect a micro-embolic effect after TheraSphere radioembolization of neuroendocrine and carcinoid liver metastasis? *Cancer Biother Radio.* 2013;28(6):459–65.
17. Sangro B, Carpanese L, Cianni R, Golfieri R, Gasparini D, Ezzidin S, et al. European multicenter evaluation of survival for patients with hepatocellular carcinoma (HCC) treated by radioembolization with 90y-labeled resin microspheres. *J Clin Oncol.* 2010;28(15_suppl):4027.
18. Riaz A, Lewandowski RJ, Kulik LM, Mulcahy MF, Sato KT, Ryu RK, et al. Complications following radioembolization with yttrium-90 microspheres: a comprehensive literature review. *J Vasc Interv Radiol.* 2009;20(9):1121–30; quiz 31.
19. Gulec SA, Siegel JA. Posttherapy radiation safety considerations in radiomic sphere treatment with 90Y-microspheres. *J Nucl Med.* 2007;48(12):2080–6.
20. Giammarile F, Bodei L, Chiesa C, Flux G, Forrer F, Kraeber-Bodere F, et al. EANM procedure guideline for the treatment of liver cancer and liver metastases

- with intra-arterial radioactive compounds. *Eur J Nucl Med Mol Imaging*. 2011;38(7):1393–406.
21. Jernigan SR, Osborne JA, Mirek CJ, Buckner G. Selective internal radiation therapy: quantifying distal penetration and distribution of resin and glass microspheres in a surrogate arterial model. *J Vasc Interv Radiol*. 2015;26(6):897–904 e2.
 22. Gray B, Van Hazel G, Hope M, Burton M, Moroz P, Anderson J, et al. Randomised trial of SIR-Spheres plus chemotherapy vs. chemotherapy alone for treating patients with liver metastases from primary large bowel cancer. *Ann Oncol*. 2001;12(12):1711–20.
 23. Carr BI. Hepatic arterial ⁹⁰Yttrium glass microspheres (Therasphere) for unresectable hepatocellular carcinoma: interim safety and survival data on 65 patients. *Liver Transpl*. 2004;10(2 Suppl 1):S107–10.
 24. Van Hazel G, Blackwell A, Anderson J, Price D, Moroz P, Bower G, et al. Randomised phase 2 trial of SIR-spheres plus fluorouracil/leucovorin chemotherapy versus fluorouracil/leucovorin chemotherapy alone in advanced colorectal cancer. *J Surg Oncol*. 2004;88(2):78–85.
 25. Sangro B, Bilbao JJ, Boan J, Martinez-Cuesta A, Benito A, Rodriguez J, et al. Radioembolization using ⁹⁰Y-resin microspheres for patients with advanced hepatocellular carcinoma. *Int J Radiat Oncol Biol Phys*. 2006;66(3):792–800.
 26. Garin E, Rolland Y, Boucher E, Ardisson V, Laffont S, Boudjema K, et al. First experience of hepatic radioembolization using microspheres labelled with yttrium-90 (TheraSphere): practical aspects concerning its implementation. *Eur J Nucl Med Mol Imaging*. 2010;37(3):453–61.
 27. Prince JF, Smits ML, Krijger GC, Zonnenberg BA, van den Bosch MA, Nijsen JF, et al. Radiation emission from patients treated with holmium-166 radioembolization. *J Vasc Interv Radiol*. 2014;25(12):1956–63 e1.
 28. Smits ML, Elschot M, van den Bosch MA, van de Maat GH, van het Schip AD, Zonnenberg BA, et al. In vivo dosimetry based on SPECT and MR imaging of ¹⁶⁶Ho-microspheres for treatment of liver malignancies. *J Nucl Med*. 2013;54(12):2093–100.
 29. Smits ML, Nijsen JF, van den Bosch MA, Lam MG, Vente MA, Mali WP, et al. Holmium-166 radioembolisation in patients with unresectable, chemorefractory liver metastases (HEPAR trial): a phase 1, dose-escalation study. *Lancet Oncol*. 2012;13(10):1025–34.
 30. Reinders MTM, Smits MLJ, van Roekel C, Braat A. Holmium-166 microsphere radioembolization of hepatic malignancies. *Semin Nucl Med*. 2019;49(3):237–43.
 31. Wunderlich G, Pinkert J, Andreeff M, Stintz M, Knapp FF Jr, Kropp J, et al. Preparation and biodistribution of rhenium-188 labeled albumin microspheres B 20: a promising new agent for radiotherapy. *Appl Radiat Isot*. 2000;52(1):63–8.
 32. Mallia MB, Chirayil V, Dash A. Improved freeze-dried kit for the preparation of (188)ReN-DEDC/lipiodol for the therapy of unresectable hepatocellular carcinoma. *Appl Radiat Isot*. 2018;137:147–53.
 33. Nowicki ML, Cwikla JB, Sankowski AJ, Shcherbinin S, Grimmes J, Celler A, et al. Initial study of radiological and clinical efficacy radioembolization using ¹⁸⁸Re-human serum albumin (HSA) microspheres in patients with progressive, unresectable primary or secondary liver cancers. *Med Sci Monit*. 2014;20:1353–62.
 34. Jeong JM, Kim YJ, Lee YS, Ko JI, Son M, Lee DS, et al. Lipiodol solution of a lipophilic agent, (188) Re-TDD, for the treatment of liver cancer. *Nucl Med Biol*. 2001;28(2):197–204.
 35. Boschi A, Uccelli L, Duatti A, Colamussi P, Cittanti C, Filice A, et al. A kit formulation for the preparation of ¹⁸⁸Re-lipiodol: preclinical studies and preliminary therapeutic evaluation in patients with unresectable hepatocellular carcinoma. *Nucl Med Commun*. 2004;25(7):691–9.
 36. Kumar A, Srivastava DN, Chau TT, Long HD, Bal C, Chandra P, et al. Inoperable hepatocellular carcinoma: transarterial ¹⁸⁸Re HDD-labeled iodized oil for treatment – prospective multicenter clinical trial. *Radiology*. 2007;243(2):509–19.
 37. Raoul JL, Bourguet P, Bretagne JF, Duvauferrier R, Coornaert S, Darnault P, et al. Hepatic artery injection of I-131-labeled lipiodol. Part I. Biodistribution study results in patients with hepatocellular carcinoma and liver metastases. *Radiology*. 1988;168(2):541–5.
 38. Park CH, Suh JH, Yoo HS, Lee JT, Kim DI. Evaluation of intrahepatic I-131 ethiodol on a patient with hepatocellular carcinoma. Therapeutic feasibility study. *Clin Nucl Med*. 1986;11(7):514–7.
 39. Yoo HS, Lee JT, Kim KW, Kim BS, Choi HJ, Lee KS, et al. Nodular hepatocellular carcinoma. Treatment with subsegmental intraarterial injection of iodine 131-labeled iodized oil. *Cancer*. 1991;68(9):1878–84.
 40. Kobayashi H, Hidaka H, Kajiya Y, Tanoue P, Inoue H, Ikeda K, et al. Treatment of hepatocellular carcinoma by transarterial injection of anticancer agents in iodized oil suspension or of radioactive iodized oil solution. *Acta Radiol Diagn (Stockh)*. 1986;27(2):139–47.
 41. Raoul JL, Guyader D, Bretagne JF, Duvauferrier R, Bourguet P, Bekhechi D, et al. Randomized controlled trial for hepatocellular carcinoma with portal vein thrombosis: intra-arterial iodine-131-iodized oil versus medical support. *J Nucl Med*. 1994;35(11):1782–7.
 42. Ahmadzadehfar H, Sabet A, Wilhelm K, Biersack HJ, Risse J. Iodine-131-lipiodol therapy in hepatic tumours. *Methods*. 2011;55(3):246–52.
 43. Toohey RE, Stabin MG, Watson EE. The AAPM/RSNA physics tutorial for residents: internal radiation dosimetry: principles and applications. *Radiographics*. 2000;20(2):533–46; quiz 1–2.
 44. Fox RA, Klemp PF, Egan G, Mina LL, Burton MA, Gray BN. Dose distribution following selective internal radiation therapy. *Int J Radiat Oncol Biol Phys*. 1991;21(2):463–7.
 45. Liu DM, Westcott M, Garcia-Monacp R, Abraham R, Gandhi R. Down and dirty with dosimetry. *Endovascular Today*. 2016;15(9):70–6.
 46. Spreafico C, Morosi C, Maccauro M, Romito R, Lanocita R, Civelli EM, et al. Intrahepatic flow redis-

- tribution in patients treated with radioembolization. *Cardiovasc Intervent Radiol.* 2015;38(2):322–8.
47. Ho S, Lau WY, Leung TW, Chan M, Ngar YK, Johnson PJ, et al. Partition model for estimating radiation doses from yttrium-90 microspheres in treating hepatic tumours. *Eur J Nucl Med.* 1996;23(8):947–52.
 48. Kennedy AS, Kleinstreuer C, Basciano CA, Dezarn WA. Computer modeling of yttrium-90-microsphere transport in the hepatic arterial tree to improve clinical outcomes. *Int J Radiat Oncol Biol Phys.* 2010;76(2):631–7.
 49. Wasan HS, Gibbs P, Sharma NK, Taieb J, Heinemann V, Ricke J, et al. First-line selective internal radiotherapy plus chemotherapy versus chemotherapy alone in patients with liver metastases from colorectal cancer (FOXFIRE, SIRFLOX, and FOXFIRE-Global): a combined analysis of three multicentre, randomised, phase 3 trials. *Lancet Oncol.* 2017;18(9):1159–71.
 50. Sangro B, Gil-Alzugaray B, Rodriguez J, Sola I, Martinez-Cuesta A, Viudez A, et al. Liver disease induced by radioembolization of liver tumors: description and possible risk factors. *Cancer.* 2008;112(7):1538–46.
 51. Kennedy AS, McNeillie P, Dezarn WA, Nutting C, Sangro B, Wertman D, et al. Treatment parameters and outcome in 680 treatments of internal radiation with resin 90Y-microspheres for unresectable hepatic tumors. *Int J Radiat Oncol Biol Phys.* 2009;74(5):1494–500.
 52. Gulec SA, Mesoloras G, Stabin M. Dosimetric techniques in 90Y-microsphere therapy of liver cancer: the MIRD equations for dose calculations. *J Nucl Med.* 2006;47(7):1209–11.
 53. Gandhi M, Choo SP, Thng CH, Tan SB, Low AS, Cheow PC, et al. Single administration of Selective Internal Radiation Therapy versus continuous treatment with sorafenib in locally advanced hepatocellular carcinoma (SIRveNIB): study protocol for a phase iii randomized controlled trial. *BMC Cancer.* 2016;16(1):856.
 54. Cremonesi M, Chiesa C, Strigari L, Ferrari M, Botta F, Guerriero F, et al. Radioembolization of hepatic lesions from a radiobiology and dosimetric perspective. *Front Oncol.* 2014;4:210.
 55. Carretero C, Munoz-Navas M, Betes M, Angos R, Subtil JC, Fernandez-Urrien I, et al. Gastrointestinal injury after radioembolization of hepatic tumors. *Am J Gastroenterol.* 2007;102(6):1216–20.
 56. Kennedy A, Nag S, Salem R, Murthy R, McEwan AJ, Nutting C, et al. Recommendations for radioembolization of hepatic malignancies using yttrium-90 microsphere brachytherapy: a consensus panel report from the radioembolization brachytherapy oncology consortium. *Int J Radiat Oncol Biol Phys.* 2007;68(1):13–23.
 57. Salem R, Thurston KG. Radioembolization with yttrium-90 microspheres: a state-of-the-art brachytherapy treatment for primary and secondary liver malignancies: part 3: comprehensive literature review and future direction. *J Vasc Interv Radiol.* 2006;17(10):1571–93.
 58. Ahmadzadehfar H, Duan H, Haug AR, Walrand S, Hoffmann M. The role of SPECT/CT in radioembolization of liver tumours. *Eur J Nucl Med Mol Imaging.* 2014;41 Suppl 1:S115–24.
 59. Dewaraja YK, Frey EC, Sgouros G, Brill AB, Roberson P, Zanzonico PB, et al. MIRD pamphlet No. 23: quantitative SPECT for patient-specific 3-dimensional dosimetry in internal radionuclide therapy. *J Nucl Med.* 2012;53(8):1310–25.
 60. J OD. A review of 3D image-based dosimetry, technical considerations and emerging perspectives in (90)Y microsphere therapy. *J Diagn Imaging Ther.* 2015;2(2):1–34.
 61. Mikell JK, Dewaraja YK, Owen D. Transarterial radioembolization for hepatocellular carcinoma and hepatic metastases: clinical aspects and dosimetry models. *Semin Radiat Oncol.* 2020;30(1):68–76.
 62. Lhommel R, Goffette P, Van den Eynde M, Jamar F, Pauwels S, Bilbao JI, et al. Yttrium-90 TOF PET scan demonstrates high-resolution biodistribution after liver SIRT. *Eur J Nucl Med Mol Imaging.* 2009;36(10):1696.
 63. Selwyn RG, Nickles RJ, Thomadsen BR, DeWerd LA, Micka JA. A new internal pair production branching ratio of 90Y: the development of a non-destructive assay for 90Y and 90Sr. *Appl Radiat Isot.* 2007;65(3):318–27.
 64. Carlier T, Willowson KP, Fourkal E, Bailey DL, Doss M, Conti M. (90)Y -PET imaging: exploring limitations and accuracy under conditions of low counts and high random fraction. *Med Phys.* 2015;42(7):4295–309.
 65. Willowson KP, Tapner M, Team QI, Bailey DL. A multicentre comparison of quantitative (90)Y PET/CT for dosimetric purposes after radioembolization with resin microspheres: the QUEST Phantom Study. *Eur J Nucl Med Mol Imaging.* 2015;42(8):1202–22.
 66. Shah RP, Sze DY. Radioembolization: identifying and managing anatomic variants. In: Bilbao JI, Reiser MF, editors. *Liver Radioembolization with 90Y microspheres.* Medical radiology. Berlin, Heidelberg: Springer Berlin Heidelberg; 2013. p. 41–52.
 67. Samuelson SD, Louie JD, Sze DY. N-butyl cyanoacrylate glue embolization of arterial networks to facilitate hepatic arterial skeletonization before radioembolization. *Cardiovasc Intervent Radiol.* 2013;36(3):690–8.
 68. McWilliams JP, Kee ST, Loh CT, Lee EW, Liu DM. Prophylactic embolization of the cystic artery before radioembolization: feasibility, safety, and outcomes. *Cardiovasc Intervent Radiol.* 2011;34(4):786–92.
 69. Inaba Y, Arai Y, Matsueda K, Takeuchi Y, Aramaki T. Right gastric artery embolization to prevent acute gastric mucosal lesions in patients undergoing repeat hepatic arterial infusion chemotherapy. *J Vasc Interv Radiol.* 2001;12(8):957–63.
 70. Wang DS, Louie JD, Kothary N, Shah RP, Sze DY. Prophylactic topically applied ice to prevent cutaneous complications of nontarget chemoemboli-

- zation and radioembolization. *J Vasc Interv Radiol*. 2013;24(4):596–600.
71. Bilbao JI, Garrastachu P, Herraiz MJ, Rodriguez M, Inarrairaegui M, Rodriguez J, et al. Safety and efficacy assessment of flow redistribution by occlusion of intrahepatic vessels prior to radioembolization in the treatment of liver tumors. *Cardiovasc Intervent Radiol*. 2010;33(3):523–31.
 72. Kim HC. Radioembolization for the treatment of hepatocellular carcinoma. *Clin Mol Hepatol*. 2017;23(2):109–14.
 73. Gates VL, Marshall KG, Salzig K, Williams M, Lewandowski RJ, Salem R. Outpatient single-session yttrium-90 glass microsphere radioembolization. *J Vasc Interv Radiol*. 2014;25(2):266–70.
 74. Liapi E, Geschwind JFH. Radioembolization for hepatocellular carcinoma. In: Mauro MA, Murphy K, Thomson KR, Venbrux AC, Morgan RA, editors. *Image-guided interventions*; Saunders/Elsevier Philadelphia, PA. 2014. p. 441–9.
 75. Arbizu J, Rodriguez-Fraile M, Martí-Climent JM, Domínguez-Prado I, Vigil C. Nuclear medicine procedures for treatment evaluation and administration. In: Bilbao JI, Reiser MF, editors. *Liver radioembolization with 90Y microspheres*. Medical radiology. Berlin, Heidelberg: Springer Berlin Heidelberg; 2013. p. 63–75.
 76. Ahmadzadehfar H, Muckle M, Sabet A, Wilhelm K, Kuhl C, Biermann K, et al. The significance of bremsstrahlung SPECT/CT after yttrium-90 radioembolization treatment in the prediction of extrahepatic side effects. *Eur J Nucl Med Mol Imaging*. 2012;39(2):309–15.
 77. Ward TJ, Tamrazi A, Lam MG, Louie JD, Kao PN, Shah RP, et al. Management of high hepatopulmonary shunting in patients undergoing hepatic radioembolization. *J Vasc Interv Radiol*. 2015;26(12):1751–60.
 78. Kulik LM, Carr BI, Mulcahy MF, Lewandowski RJ, Atassi B, Ryu RK, et al. Safety and efficacy of 90Y radiotherapy for hepatocellular carcinoma with and without portal vein thrombosis. *Hepatology*. 2008;47(1):71–81.
 79. Lingiah VA, Niazi M, Olivo R, Paterno F, Guarrera JV, Pysopoulos NT. Liver transplantation beyond Milan criteria. *J Clin Transl Hepatol*. 2020;8(1):69–75.
 80. O’Leary C, Mahler M, Soulen MC. Curative-intent therapies in localized hepatocellular carcinoma. *Curr Treat Options in Oncol*. 2020;21(4):31.
 81. Somma F, Stoaia V, Serra N, D’Angelo R, Gatta G, Fiore F. Yttrium-90 trans-arterial radioembolization in advanced-stage HCC: the impact of portal vein thrombosis on survival. *PLoS One*. 2019;14(5):e0216935.
 82. Gabr A, Polineni P, Mouli SK, Riaz A, Lewandowski RJ, Salem R. Neoadjuvant radiation lobectomy as an alternative to portal vein embolization in hepatocellular carcinoma. *Semin Nucl Med*. 2019;49(3):197–203.
 83. Kessler J, Park JJ. Yttrium-90 radioembolization after local hepatic therapy: how prior treatments impact patient selection, dosing, and toxicity. *Tech Vasc Interv Radiol*. 2019;22(2):112–6.
 84. Zimmermann M, Schulze-Hagen M, Liebl M, Pedersoli F, Goerg F, Ulmer TF, et al. Safety and efficacy of Y-90 radioembolization after prior major hepatic resection. *Cardiovasc Intervent Radiol*. 2017;40(8):1206–12.
 85. Gil-Alzugaray B, Chopitea A, Inarrairaegui M, Bilbao JI, Rodriguez-Fraile M, Rodriguez J, et al. Prognostic factors and prevention of radioembolization-induced liver disease. *Hepatology*. 2013;57(3):1078–87.
 86. Samim M, van Veenendaal LM, Braat M, van den Hoven AF, Van Hillegersberg R, Sangro B, et al. Recommendations for radioembolisation after liver surgery using yttrium-90 resin microspheres based on a survey of an international expert panel. *Eur Radiol*. 2017;27(12):4923–30.
 87. Chen YX, Zeng ZC, Fan J, Tang ZY, Zhou J, Zeng MS, et al. Defining prognostic factors of survival after external beam radiotherapy treatment of hepatocellular carcinoma with lymph node metastases. *Clin Transl Oncol*. 2013;15(9):732–40.
 88. He J, Zeng ZC, Tang ZY, Fan J, Zhou J, Zeng MS, et al. Clinical features and prognostic factors in patients with bone metastases from hepatocellular carcinoma receiving external beam radiotherapy. *Cancer*. 2009;115(12):2710–20.
 89. Zeng ZC, Tang ZY, Fan J, Zhou J, Qin LX, Ye SL, et al. Radiation therapy for adrenal gland metastases from hepatocellular carcinoma. *Jpn J Clin Oncol*. 2005;35(2):61–7.
 90. Dawson LA, Normolle D, Balter JM, McGinn CJ, Lawrence TS, Ten Haken RK. Analysis of radiation-induced liver disease using the Lyman NTCP model. *Int J Radiat Oncol Biol Phys*. 2002;53(4):810–21.
 91. Bujold A, Massey CA, Kim JJ, Brierley J, Cho C, Wong RK, et al. Sequential phase I and II trials of stereotactic body radiotherapy for locally advanced hepatocellular carcinoma. *J Clin Oncol*. 2013;31(13):1631–9.
 92. Culleton S, Jiang H, Haddad CR, Kim J, Brierley J, Brade A, et al. Outcomes following definitive stereotactic body radiotherapy for patients with Child-Pugh B or C hepatocellular carcinoma. *Radiother Oncol*. 2014;111(3):412–7.
 93. Sandroussi C, Dawson LA, Lee M, Guindi M, Fischer S, Ghanekar A, et al. Radiotherapy as a bridge to liver transplantation for hepatocellular carcinoma. *Transpl Int*. 2010;23(3):299–306.
 94. Marrero JA, Kulik LM, Sirlin CB, Zhu AX, Finn RS, Abecassis MM, et al. Diagnosis, staging, and management of hepatocellular carcinoma: 2018 practice guidance by the American Association for the Study of Liver Diseases. *Hepatology*. 2018;68(2):723–50.
 95. Network NCC. Hepatobiliary cancers (Version 5.2020) 2020. Available from: https://www.nccn.org/professionals/physician_gls/pdf/hepatobiliary.pdf.
 96. Hawkins MA, Dawson LA. Radiation therapy for hepatocellular carcinoma: from palliation to cure. *Cancer*. 2006;106(8):1653–63.
 97. Mornex F, Girard N, Beziat C, Kubas A, Khodri M, Trepo C, et al. Feasibility and efficacy of high-dose

- three-dimensional-conformal radiotherapy in cirrhotic patients with small-size hepatocellular carcinoma non-eligible for curative therapies – mature results of the French Phase II RTF-1 trial. *Int J Radiat Oncol Biol Phys.* 2006;66(4):1152–8.
98. Tse RV, Hawkins M, Lockwood G, Kim JJ, Cummings B, Knox J, et al. Phase I study of individualized stereotactic body radiotherapy for hepatocellular carcinoma and intrahepatic cholangiocarcinoma. *J Clin Oncol.* 2008;26(4):657–64.
 99. Dawson LA, Guha C. Hepatocellular carcinoma: radiation therapy. *Cancer J.* 2008;14(2):111–6.
 100. Kennedy AS. Radiation oncology approaches in liver malignancies. *Am Soc Clin Oncol Educ Book.* 2014:e150–5.
 101. Hoffmann RT, Diaz-Dorransoro L, Bilbao JJ. Complications and side effects. In: Bilbao JJ, Reiser MF, editors. *Liver radioembolization with 90Y microspheres.* Medical radiology. Berlin, Heidelberg: Springer Berlin Heidelberg; 2013. p. 171–5.
 102. Gaba RC, Vanmiddlesworth KA. Chemoembolic hepatopulmonary shunt reduction to allow safe yttrium-90 radioembolization lobectomy of hepatocellular carcinoma. *Cardiovasc Intervent Radiol.* 2012;35(6):1505–11.
 103. Leung TW, Lau WY, Ho SK, Ward SC, Chow JH, Chan MS, et al. Radiation pneumonitis after selective internal radiation treatment with intra-arterial 90yttrium-microspheres for inoperable hepatic tumors. *Int J Radiat Oncol Biol Phys.* 1995;33(4):919–24.
 104. Naymagon S, Warner RR, Patel K, Harpaz N, Machac J, Weintraub JL, et al. Gastroduodenal ulceration associated with radioembolization for the treatment of hepatic tumors: an institutional experience and review of the literature. *Dig Dis Sci.* 2010;55(9):2450–8.
 105. Rodriguez-Lago I, Carretero C, Herraiz M, Subtil JC, Betes M, Rodriguez-Fraile M, et al. Long-term follow-up study of gastroduodenal lesions after radioembolization of hepatic tumors. *World J Gastroenterol.* 2013;19(19):2935–40.
 106. Kim HC, Chung JW, Lee W, Jae HJ, Park JH. Recognizing extrahepatic collateral vessels that supply hepatocellular carcinoma to avoid complications of transcatheter arterial chemoembolization. *Radiographics.* 2005;25 Suppl 1:S25–39.
 107. Lewandowski RJ, Sato KT, Atassi B, Ryu RK, Nemcek AA Jr, Kulik L, et al. Radioembolization with 90Y microspheres: angiographic and technical considerations. *Cardiovasc Intervent Radiol.* 2007;30(4):571–92.
 108. Singh P, Anil G. Yttrium-90 radioembolization of liver tumors: what do the images tell us? *Cancer Imaging.* 2014;13(4):645–57.
 109. Atassi B, Bangash AK, Lewandowski RJ, Ibrahim S, Kulik L, Mulcahy MF, et al. Biliary sequelae following radioembolization with Yttrium-90 microspheres. *J Vasc Interv Radiol.* 2008;19(5):691–7.
 110. Kobayashi S, Nakanuma Y, Terada T, Matsui O. Postmortem survey of bile duct necrosis and biloma in hepatocellular carcinoma after transcatheter arterial chemoembolization therapy: relevance to microvascular damages of peribiliary capillary plexus. *Am J Gastroenterol.* 1993;88(9):1410–5.
 111. Sakamoto I, Iwanaga S, Nagaoki K, Matsuoka Y, Ashizawa K, Uetani M, et al. Intrahepatic biloma formation (bile duct necrosis) after transcatheter arterial chemoembolization. *AJR Am J Roentgenol.* 2003;181(1):79–87.
 112. Braat MN, van Erpecum KJ, Zonnenberg BA, van den Bosch MA, Lam MG. Radioembolization-induced liver disease: a systematic review. *Eur J Gastroenterol Hepatol.* 2017;29(2):144–52.
 113. Jakobs TF, Saleem S, Atassi B, Reda E, Lewandowski RJ, Yaghmai V, et al. Fibrosis, portal hypertension, and hepatic volume changes induced by intra-arterial radiotherapy with 90yttrium microspheres. *Dig Dis Sci.* 2008;53(9):2556–63.
 114. Noshier JL, Ohman-Strickland PA, Jabbour S, Narra V, Noshier B. Changes in liver and spleen volumes and liver function after radioembolization with yttrium-90 resin microspheres. *J Vasc Interv Radiol.* 2011;22(12):1706–13.
 115. Fernandez-Ros N, Inarrairaegui M, Paramo JA, Berasain C, Avila MA, Chopitea A, et al. Radioembolization of hepatocellular carcinoma activates liver regeneration, induces inflammation and endothelial stress and activates coagulation. *Liver Int.* 2015;35(5):1590–6.
 116. Marn CS, Andrews JC, Francis IR, Hollett MD, Walker SC, Ensminger WD. Hepatic parenchymal changes after intraarterial Y-90 therapy: CT findings. *Radiology.* 1993;187(1):125–8.
 117. Therasse P, Arbuck SG, Eisenhauer EA, Wanders J, Kaplan RS, Rubinstein L, et al. New guidelines to evaluate the response to treatment in solid tumors. European Organization for Research and Treatment of Cancer, National Cancer Institute of the United States, National Cancer Institute of Canada. *J Natl Cancer Inst.* 2000;92(3):205–16.
 118. Bruix J, Sherman M, Llovet JM, Beaugrand M, Lencioni R, Burroughs AK, et al. Clinical management of hepatocellular carcinoma. Conclusions of the Barcelona-2000 EASL conference. European Association for the Study of the Liver. *J Hepatol.* 2001;35(3):421–30.
 119. Riaz A, Kulik L, Lewandowski RJ, Ryu RK, Giakoumis Spear G, Mulcahy MF, et al. Radiologic-pathologic correlation of hepatocellular carcinoma treated with internal radiation using yttrium-90 microspheres. *Hepatology.* 2009;49(4):1185–93.
 120. Rhee TK, Naik NK, Deng J, Atassi B, Mulcahy MF, Kulik LM, et al. Tumor response after yttrium-90 radioembolization for hepatocellular carcinoma: comparison of diffusion-weighted functional MR imaging with anatomic MR imaging. *J Vasc Interv Radiol.* 2008;19(8):1180–6.